

RSC Advances



This is an *Accepted Manuscript*, which has been through the Royal Society of Chemistry peer review process and has been accepted for publication.

Accepted Manuscripts are published online shortly after acceptance, before technical editing, formatting and proof reading. Using this free service, authors can make their results available to the community, in citable form, before we publish the edited article. This *Accepted Manuscript* will be replaced by the edited, formatted and paginated article as soon as this is available.

You can find more information about *Accepted Manuscripts* in the [Information for Authors](#).

Please note that technical editing may introduce minor changes to the text and/or graphics, which may alter content. The journal's standard [Terms & Conditions](#) and the [Ethical guidelines](#) still apply. In no event shall the Royal Society of Chemistry be held responsible for any errors or omissions in this *Accepted Manuscript* or any consequences arising from the use of any information it contains.

Ultrasound-Assisted Bioalcohol Synthesis: Review and Analysis

Amrita Ranjan,^{1,2,#} Shuchi Singh,^{1,#} Ritesh S. Malani^{1,#} and Vijayanand S. Moholkar^{1,3,*}

¹ Center for Energy, Indian Institute of Technology Guwahati, Guwahati – 781 039, Assam, India

² Instituto de Biología Molecular y Celular de Plantas (IBMCP), UPV – CSIC, Ciudad Politécnica de la Innovación, Ingeniero Fausto Elio, s/n 46022 Valencia – Spain

³ Department of Chemical Engineering, Indian Institute of Technology Guwahati, Guwahati – 781 039, Assam, India

Equal contribution by these authors

* Author for correspondence. Fax: +91 361 258 2291. E-mail: vmoholkar@iitg.ernet.in

Abstract

Sonication (or ultrasound irradiation) has emerged as potential technique for intensification of diverse physical/ chemical/ biological processes. In recent years, sonication has been applied in synthesis of liquid biofuels such as biodiesel and bioalcohol such as ethanol. The process of synthesis of bioalcohols comprises of four steps, viz. acid pretreatment, alkaline delignification, enzymatic hydrolysis and fermentation. Significant literature has been published in past one decade on application of ultrasound for intensification of all steps of bioalcohol synthesis. In this paper, a critical review and analysis of the literature on ultrasound-assisted bioalcohol synthesis has been presented. This review has addressed all four steps of bioalcohol synthesis. Essentially, literature in the area of ultrasound-assisted biomass pretreatment, delignification and hydrolysis has been reviewed, followed by analysis of literature on ultrasound-assisted fermentation. Finally, a review of the mechanistic investigations in various steps of bioalcohol synthesis has been given that has highlighted synergistic links between physical/chemical effects of ultrasound and cavitation, and the basic physical/chemical mechanism of various steps of bioalcohol synthesis. The critical analysis of literature in this review has not only demonstrated the efficacy of ultrasound in intensification of all steps of bioalcohol synthesis, but has also brought to light the underlying mechanistic issues, which could form guidelines for design and optimization of commercial scale bioalcohol process.

Keywords: Ultrasound, Cavitation, Pretreatment, Hydrolysis, Delignification, Biomass, Fermentation, Bioalcohol

1. Introduction

Fast depletion of global fossil fuel reserves has made energy security a daunting issue for several developing economies, especially those like India which are heavily dependent on import of crude oil. Another concern is that of climate change risk and environmental pollution due to enormous rise in emissions of greenhouse gases and particulate matter from vehicular exhaust. As a consequence, past two decades have witnessed intense research activity in both academic institutions and industrial R&D units focused on alternate renewable liquid transportation fuel. Both thermo-chemical and biochemical routes of conversion of biomass to liquid fuel have been extensively explored. Additional options for renewable liquid transportation fuel are the alcoholic fuels such as ethanol and butanol ¹, which can be blended with petrol or gasoline. These alcohols are produced from fermentation of hexose and pentose sugars. In category of alcoholic biofuels, the most popular fuel is ethanol, which conventionally is a major byproduct of the sugar industry. However, the substrate for ethanol, *i.e.* molasses, has numerous other outlets like beverage industry and distilleries that pay higher price. The sugar industry prefers to sell molasses for potable use, which fetches high revenue. Thus, the ethanol from sugar industry is largely unavailable for blending with gasoline. This necessitates exploration of alternate sources of ethanol derived through cheaper substrates. Lignocellulosic biomass available in the form of agro-residue or forest-residue or waste biomasses like invasive weeds and grasses are potential substrates for bioethanol production. These biomasses have significant content of cellulose and hemicellulose, which can be converted to fermentable pentose/hexose sugars after pretreatment and enzyme hydrolysis. However, major bottleneck of commercial scale bioalcohol production from this route is the high cost of biomass pretreatment and hydrolysis. This necessitates quest for simple, energy efficient and low-cost technology for effective biomass pretreatment. Another hurdle in large scale commercial production of bioalcohol is the slow kinetics of fermentation, which puts severe restriction on the rate of production. These two issues hamper large-scale production of bioalcohols and economic

feasibility, despite their promise for mitigating the threats of energy security and climate change risk. Process intensification is a possible solution to these problems related to large-scale production of bioalcohols.

The basis for intensification of any process (whether physical, chemical or biological) is to explore and establish new and efficient methods of introduction of energy into the system to bring about the required transformation with higher yield and kinetics. Among several methods of process intensification that have emerged in past three decades one is “sonication”, or ultrasound irradiation of the process (or reaction) system. Basically, ultrasound wave is a longitudinal wave that passes through any compressible medium in the form of compression and rarefaction cycle. The molecules or fluid elements of the medium are set in oscillatory motion due to propagation of the ultrasound wave. The frequency range of the ultrasound wave is 20 kHz to about 10 MHz. As ultrasound propagates through the medium in the form of compression/rarefaction cycles, the static pressure in the medium undergoes periodic (typically sinusoidal) variation. This variation can lead to occurrence of *cavitation phenomenon* in the medium. Cavitation phenomenon basically involves nucleation, volumetric oscillations and implosive collapse of tiny gas or vapor bubbles, which is driven by the variation in static pressure induced by ultrasound wave. The major peculiarity of phenomenon of transient cavitation is that it causes extreme energy concentration in the medium at an incredibly small temporal (~ 50 ns) and spatial scale (~ 100 nm).² During transient implosive collapse of the bubble, the temperature and pressure inside the bubble reach extremely high values (~ 5000 K and ~ 50 MPa).^{3, 4} Energy concentration created by transient cavitation has both physical and chemical implications on the reaction system. The physical effect of ultrasound and cavitation is the generation of intense micro-mixing (or local convection) in the medium through different mechanisms, viz. microstreaming, acoustic streaming, microturbulence, acoustic waves and microjets. This convection helps towards enhancing the mass transfer in the system. Chemical effect associated with transient collapse of the cavitation bubble is essentially generation of

highly reactive radical species. These species are generated by thermal dissociation of the gas and vapor molecules entrapped in the bubble at the moment of transient collapse. The cavitation bubble may get fragmented at the instance of maximum compression (or minimum radius) during radial motion. At this moment, all chemical species inside the bubble – including radical species - get released into the medium where they can induce / accelerate chemical reactions. This is the well known sonochemical effect. Ultrasound-assisted intensification of synthesis of different types of biofuels has been an active area of research for past one decade, and voluminous literature has been published in this area. Greater details on the basics of ultrasound wave phenomena and cavitation bubble dynamics (and associated heat/mass transfer effects) have been given in the supplementary information provided with this paper.

An excellent and comprehensive review of this literature has been recently published by Luo *et al.*⁵ Main biofuels processes that have been studied for ultrasound assisted intensification include: (1) pretreatment of lignocellulosic biomass (delignification under alkaline treatment/dilute acid hydrolysis), (2) enzymatic hydrolysis (or saccharification) of pretreated (cellulose rich) biomass, (3) fermentation of the pentose/hexose rich hydrolyzates from acid/enzymatic hydrolysis to bioalcohols (mainly ethanol and butanol), (4) microalgal lipid extraction, (5) biodiesel synthesis using homogeneous (acid/alkali), heterogeneous and enzyme catalyst, and (6) biogas digestion.⁶

Most of the literature published in the area of ultrasound-assisted biofuels synthesis has focused on the results than rationale. Previous authors have accounted for beneficial effect of ultrasound in terms of enhancement in the yield of the process, faster kinetics or reduction in the number of processing steps in the process. However, little effort is given in these studies towards deduction of the exact physical mechanism underlying ultrasound-induced enhancement of the process.⁶ Essentially, relative contributions of physical and chemical effects of ultrasound and cavitation (noted earlier) towards enhancement of the process have not been identified. Mechanistic investigations are crucial for effective scale-up of the process, as they give an

insight into the relative influence of all parameters on the gross outcome of the process and form guidelines for the optimization of these parameters.

1.1 Aim and scope of this review

The purpose of this review is to give a critical account of the literature published in the area of ultrasound assisted synthesis of bioalcohols. Since the bioalcohol process also includes the steps of biomass pretreatment, this review also includes analysis of literature on ultrasound assisted pretreatment of biomass including dilute acid hydrolysis, alkaline delignification and enzymatic hydrolysis. The major objectives of this review are not only to present the summaries and overview of the literature in the area of ultrasound assisted biomass pretreatment and fermentation, but also to analyze the literature from mechanistic viewpoint. This essentially means that we make an attempt to identify the exact role played by ultrasound and cavitation in enhancement of the pretreatment/ fermentation process from the results reported in literature, which could be in the form of increase in kinetics or yield of the process or use of cruder enzymes, non-optimum conditions of pretreatment / hydrolysis / fermentation. In other words, in this review we have made an attempt to establish the synergy between basic physics / chemistry of the process, and the physical and chemical effects of ultrasound and cavitation, and this could be a peculiar feature of this review.

2. Ultrasound in biomass pretreatment

Bioprocesses for production of alcoholic fuels comprise of three steps, viz. (i) biomass pretreatment (acid hydrolysis and delignification), (ii) enzymatic hydrolysis of pretreated biomass, and (iii) fermentation of the hydrolyzates obtained from acid and enzymatic hydrolysis, which are rich in pentose and hexose sugars, respectively. The first step of this chain is not only crucially important as it directly influences the production rate of alcohol, but is also cost intensive. The biomass pretreatment is aimed at removal of lignin and hemicellulose components from biomass. Numerous low-cost pretreatments have been developed for

lignocellulosic biomass, which include physical, chemical, biological techniques and combinations thereof. The best possible pretreatment method is substrate specific. The main criteria used for choosing the optimum pretreatment method for a particular feedstock are: (i) preserving cellulosic and hemicellulosic fractions during treatment, (ii) limitations of formation of side products due to degradation/ oxidation of cellulose/ hemicellulose (i.e. to avoid the oxidation of reducible sugars to furfural and other inhibitory products for cell growth and fermentation), (iii) minimum energy input, and (iv) cost effectiveness. In this section, we have presented a consolidated review of literature in the area of ultrasound-assisted biomass pretreatment. However, prior to it, we have given below a brief description of the most common techniques used for pretreatment of biomass.^{7,8}

2.1 Physical and physico-chemical pretreatments

This treatment is essentially aimed at particle size reduction of biomass. The common techniques employed in this treatment are milling, irradiation (either gamma ray, electron beam, microwave etc.) and extrusion. Reduction in biomass particle size (leading to enhanced mass transfer) and reduction in crystallinity enhances yield and kinetics of enzymatic hydrolysis.

Physico-chemical pretreatments: These treatments combine both physical and chemical techniques. Some important pretreatments in this category are steam explosion, ammonia fiber explosion and liquid hot water treatment. Steam explosion is aimed at explosive decomposition of biomass by treatment with high pressure steam followed by sudden reduction in pressure. Steam explosion causes swelling of the biomass that increases its porosity. Moreover, this process also involves in-situ formation of acids that catalyze hydrolysis of soluble hemicellulose oligomers. Ammonia fiber explosion (AFEX) is a similar physico-chemical treatment as steam explosion. In this case, biomass is exposed to liquid ammonia at high temperature and pressure, followed by sudden reduction in pressure. The AFEX treatment has several beneficial effects such as reduction in cellulose crystallinity, depolymerization of hemicellulose, cleavage of lignin-carbohydrate linkages and lignin C-O-C bond, structure disruption and swelling of

biomass leading to higher surface area and enhancement in wettability. An extension of AFEX treatment is supercritical CO₂ explosion. This technique has distinct merits such as operation at lower temperature, lesser degradation of sugars and lower formation of inhibitory compounds. Moreover, this technique is more economic than AFEX due to low cost of CO₂. Liquid hot water pretreatment essentially utilizes water in liquid state at elevated temperature and pressure for treatment of biomass, where biomass undergoes “cooking”. The liquid hot water pretreatment has several merits such as enhancement of cellulose digestibility, sugar (pentose) extraction and recovery, and no formation of inhibitor compounds from oxidation of cellulose/ hemicellulose. The principal difference between liquid hot water pretreatment and steam pretreatment is the concentration of solubilized products in the solution. Liquid hot water pretreatment achieves higher total amount of the solubilized products, although at relatively lower concentrations than steam pretreatment due to larger quantities of water used in the treatment. Liquid hot water treatment also yields higher concentrations of xylose sugars. However, at higher concentration of solids, some of the monomeric xylenes may be departed to furfural.

2.2 Chemical pretreatments

The common chemical pretreatments for lignocellulosic biomass include: (i) ozonolysis, (ii) acid hydrolysis, (iii) alkaline hydrolysis, (iv) oxidative delignification, and (v) organosolv processes. A brief description of each of these processes is given below:

Ozonolysis: Ozone treatment is essentially oxidative degradation of lignin. This treatment is usually carried out under aqueous or hydrated conditions, which gives more effective oxidation. Along with lignin, a small fraction of hemicellulose is also degraded, but cellulose is not affected.

Acid hydrolysis: The acid pretreatment of biomass involves agitation/ mixing of biomass in either concentrated or dilute acid solution at elevated temperature (130-210°C). The acid concentration during treatments varies from 0.2–2.5 wt%. Conventionally, dilute sulfuric acid is used for pretreatment; although over acids like phosphoric acid, hydrochloric acid and nitric acid

have also been used. Dilute acid pretreatment effectively breaks down the rigid structure of lignocellulosic material and hydrolyzes the hemicellulosic fraction of biomass to pentose (xylose) sugars. For higher acid concentrations, the xylose sugars are further degraded to furfural. Acid pretreatment also increases the porosity of the biomass, which aids its digestibility during enzyme hydrolysis. Dilute acid pretreatment is also revealed to hydrolyze the amorphous fraction of cellulose to hexose sugars leaving behind the crystalline cellulose fraction.

Alkaline hydrolysis: The alkaline pretreatment or hydrolysis is aimed at removal of the lignin fraction of the biomass. Typical bases employed during alkaline hydrolysis include NaOH, KOH, Ca(OH)₂ and NH₄OH. The main physical/chemical changes induced by alkaline treatment include degradation of ester and glycosidic side chains resulting in structural alteration/degradation of lignin, partial de-crystallization/de-polymerization and swelling of cellulose fraction and partial hydrolysis of hemicellulose fraction of biomass. Breaking of the lignin structure during alkali treatment increases the accessibility of cellulose and hemicellulose fraction to enzymes during hydrolysis. Unlike acid pretreatment, the alkaline treatment can be carried out at ambient conditions. However, elevated temperatures are usually employed to enhance the kinetics of the process.

Oxidative delignification: Delignification can also be achieved by enzymatic treatment with peroxidase enzyme in presence of H₂O₂. For a typical concentration of 2 wt% H₂O₂, treatment at ambient temperature of 30°C can remove more than 50% lignin. Moreover, pretreatment of lignocellulosic biomass with H₂O₂ also enhances its proneness towards enzymatic hydrolysis. Another variant in this category is the wet oxidation combined with addition of base, which rapidly oxidizes the lignin from lignocellulosic biomasses like wheat straw. This alternative reduces the formation of furfural or hydroxymethyl furfural, which are known inhibitors of microbial growth.

Organosolv process: The organo-solvation process involves use of mixture of organic or aqueous organic solvent with inorganic acid catalysts such as HCl or H₂SO₄ to disrupt the

internal lignin/ hemicellulose bonds. Solvents commonly used in the process are methanol, ethanol or ethylene glycol. Depending on the biomass, organic acids can also be used in the process. Typical operating conditions are temperature = 180°-195°C, ethanol concentration = 35-70% w/w and acidic pH of 2-4. Organosolv treatment effectively hydrolyzes hemicellulose to oligo- and mono-saccharides, while lignin is hydrolyzed into low molecular weight fragments that dissolve in aqueous ethanol liquor. Essentially, organosolv process involves simultaneous prehydrolysis and delignification of lignocellulosic biomass supported by organic solvents and dilute aqueous acid solutions.

Green Solvents (ionic liquids): Ionic liquids are new class of solvents that are in liquid (fluid) state at room temperature and consist entirely of ionic species. The thermodynamics and kinetics of reactions conducted in ionic liquids are different to those in conventional molecular solvents. Ionic liquids comprise of a salt where one ion is large, and the cation has low degree of symmetry. This feature reduces the lattice energy of the crystalline form of the salt and lowers the melting point. Ionic liquids are efficient solvents for degradation of lignocellulosic materials. The cellulosic materials regenerated from ionic liquids have more amorphous character and prone to degradation by cellulase. In addition, ionic liquids are less energy intensive, easy to operate and environment friendly.

Previous literature studies reports all kinds of pretreatments combined with ultrasound. The synergistic effect of conventional pretreatment and the physical/chemical effects of ultrasound and cavitation boost both kinetics and yields of different pretreatment processes. Tables 1, 2 and 3 summarize the studies in 3-steps of ultrasound-assisted biomass pretreatments, viz. dilute acid hydrolysis, alkaline delignification and enzymatic hydrolysis. The literature summary presented in Tables 1, 2 and 3 depicts numerous manifestations of the physical/chemical effects of ultrasound and cavitation on 3-steps of biomass pretreatment summarized as follows: (1) Faster and greater removal of lignin during alkali pretreatment, (2) rise in the yield of pentose and hexose sugars during acid and enzymatic hydrolysis, along with

faster kinetics, (3) faster solubilization of carbohydrates, (4) reduction in particle size of biomass, (5) disruption of the fibrous material in biomass, with no impact on granular starch material, (6) disruption of the protein matrix surrounding starch granules, (7) disruption of the amylase-lipid complexes, (8) reduction in intermolecular hydrogen bonding of lignocellulose that results in reduction in crystallinity, (9) increase in the activities of the cellulase/cellobiase enzymes without significant denaturation. A spectacular observation that can be made from Table 1, 2 and 3 is that above-mentioned effects are consistent for numerous biomasses with wide variation in the composition, i.e. net content of hemicellulose/cellulose/lignin. The ultrasound-assisted acid/alkali pretreatment also reduces the level of concentration of acid/alkali required during the process, and higher yields are feasible at relatively lower acid/alkali concentrations. This increases the life-time of the equipment involved in the pretreatment due to lesser corrosion. Another added benefit of this feature is that formation of inhibitors (due to oxidation of glucose/xylose) in the hydrolyzate reduces significantly, which assists faster fermentation with higher bioalcohol yield.

The extent of ultrasound-induced enhancement of pretreatment is, however, highly system specific. It depends on numerous factors such as frequency and intensity of ultrasound, the type of sonicator employed (whether bath or probe type), the geometry of the sonicator or the vessel used for pretreatment, temperature of the medium etc. Due to significant variation of these factors from one system to another, a quantitative comparison of the results of different studies is quite difficult. Among all factors listed above, the ultrasound intensity (or power) is crucially important, as it determines the amplitude of the ultrasound waves generated in the system. Most of the papers report the rated (or theoretical) power of the sonicator equipment. However, the actual acoustic power input to the system is quite different. This is determined by “acoustic impedance” of the system. The actual (or net) acoustic power delivered to the system is determined using calorimetric technique, and the acoustic pressure amplitude can be calculated using a simple procedure described by Sivasankar *et al.*⁴⁵ The nature of the cavitation

bubble dynamics – whether stable or transient – depends on the ultrasound pressure amplitude. The volumetric dissipation of the acoustic power is also an important factor, which has not been reported in most of previous literature. Due to these limitations of previous literature, deduction of the physical mechanism of ultrasound induced enhancement of biomass pretreatment is difficult.

3. Ultrasound assisted fermentation

In addition to the biomass pretreatment, ultrasound has also been used for enhancement of the fermentation of the pentose and hexose rich hydrolyzates obtained from biomass pretreatments. Previous authors have addressed the matter of ultrasound-assisted fermentation process for production of alcohols. There have been two approaches adopted in the previous studies: (1) sonication of the microbial cells (or inoculum) alone before its addition to the fermentation broth (with actual fermentation being carried out using mechanical agitation), and (2) intermittent sonication of the fermentation mixture itself all through the fermentation period. The literature in this area is quite limited as compared to that in area of ultrasound-assisted biomass pretreatment and enzymatic hydrolysis. We give below a summary of the literature:

(1) Ofori–Boateng and Lee ⁴⁶ have reported ultrasound assisted simultaneous saccharification and fermentation of pretreated oil palm fronds. Prior to fermentation, the biomass was treated with ultrasound assisted organosolv/ H₂O₂ at 32 kHz frequency and 200 W power. The ultrasound–assisted SSF process was optimized for following parameters, viz. fermentation time, temperature, solid loading, pH, and yeast concentration. Optimization was carried out using one variable at a time approach. The ranges of values for the various optimization variables were as follows: fermentation time = 30-360 min, temperature = 30°-50°C, pH = 3-7, yeast concentration = 5-20 g/L, and solid loading = 2.5-15% w/v. The maximum theoretical yield of bioethanol was determined using following equation:

$$\text{Yield}(\%) = \frac{C_{\text{Bioethanol}}}{0.51 \times f_{\text{cellulose}} \times C_{\text{substrate}} \times 1.111} \times 100 \quad (1)$$

where, $C_{\text{Bioethanol}}$ = maximum concentration of ethanol at the end of fermentation (g/L), $f_{\text{cellulose}}$ = cellulose fraction in pretreated biomass, $C_{\text{substrate}}$ = concentration of substrate at the beginning of SSF, 0.51 = theoretical conversion factor from glucose to ethanol, 1.111 = conversion factor for dehydration on polymerization to glucose. The optimum conditions for SSF have been determined as follows: incubation time = 5 h, temperature = 40°C, pH = 5, yeast concentration = 15 g/L, and solid loading = 10% w/v. The maximal bioethanol concentration at these conditions was 18.2 g/L with theoretical yield of 57% with application of sonication, a 6-fold rise in bioethanol concentration and 4-fold rise in percentage yield of bioethanol was obtained. Ofori-Boateng and Lee⁴⁶ have attributed high bioethanol yield at high solid loading and low fermentation time to sonication effects that disrupted the biomass efficiently for microorganisms to penetrate and convert sugars to bioethanol.

(2) Indra Neel *et al.*⁴⁷ have reported enhancement in glucose fermentation by *S. cerevisiae* to produce ethanol under mild conditions of sonication. Fermentation was carried out in an ultrasound bath at 40 kHz frequency and 120 W of theoretical power at two temperatures, viz. 20° and 30°C. The kinetics of fermentation was assessed using ¹³C NMR technique, as well as weight reduction of fermentation broth due to CO₂ formation. The overall reaction rate constant of fermentation was determined by fitting first order kinetics to glucose conversion profile. Microscopic analysis of the yeast cells revealed that mild sonication caused deagglomeration of the yeast cells, but no disruption of cells was observed. The kinetics constant of the fermentation process enhanced 2.3 and 2.5 fold at 30° and 20°C, respectively. Indra Neel *et al.*⁴⁷ did not observe yeast proliferation (or growth) in presence of ultrasound. Indra Neel *et al.*⁴⁷ have attributed ultrasound-induced enhancement of fermentation to several factors, viz (1) removal of ethanol from cell surface due to strong micro-stirring, (2) desorption of CO₂ from the fermentation broth, (3) changes in membrane permeability of cells, and (4) enhancement in mass

transfer in the cells. Indra Neel *et al.*⁴⁷ have also determined the energy efficiency of ethanol production process using an EROEI (Energy Return on Energy Invested) index, which was calculated as ~ 0.9 .

(3) Sulaiman *et al.*⁴⁸ studied the ethanol production from fermentation of lactose using the yeast *Kluyveromyces marxianus* (ATCC 46537) under ultrasound irradiation in a bioreactor (BIOFLO 110). Low-intensity sonication using 10%, 20% and 40% duty cycles were applied during fermentation in batch mode. Sonication of the fermentation broth was applied using a sonotrode mounted in an external chamber and the fermentation broth was continuously recirculated between the bioreactor (total capacity 7.5 L working volume 3 L) and the sonication chamber with a flow rate of 0.2 L/min. For the optimum duty cycle of 20%, final ethanol concentration of 5.20 ± 0.68 g/L was achieved, which was 3.5-fold higher than at control conditions (with mechanical agitation). Sonication at duty cycles of 10% and 20% substantially improved the biomass growth rate and final concentration relative to the control conditions, but further rise in duty cycle to 40% adversely affected the biomass growth rate and final concentration. The adverse effect of sonication at 40% duty cycle was reflected in the dissolved oxygen concentration during exponential growth, which found to be lesser than for smaller duty cycles. Pulsed ultrasound with duty cycles at all levels augmented ethanol production relative to control conditions, but the duty cycles of 10% and 20% were most effective. Sonication at 10% and 20% cycles enhanced both the extracellular and the intracellular levels of β -galactosidase enzyme. Cell viability study showed that viability progressively reduced with increasing duty cycles of sonication. Maximum reduction in cell viability was seen for ultrasound duty cycle of 40%. At the end of the fermentation, $> 65\%$ of the yeast cells retained viability in the broth.

(4) Jomdecha and Prateepasen⁴⁹ have investigated effect of pulsed ultrasound irradiation on the lag phase of *Saccharomyces cerevisiae* growth. Ultrasound of 20 kHz and 600 W maximum theoretical power was applied at power levels of 2, 8, 16, 24 and 32% with duty cycle of 10%. The total sonication period was 10 and 20 min for the two flasks holding microbial cultures.

After sonication, the flasks were incubated for 24 h at 30°C with orbital agitations of 100 rpm. For ultrasound energy density of 230 J/m³, the shortest lag duration of 4.74 h was observed, while longest lag time of 5.9 h was obtained for ultrasound energy input of 918 J/m³. The highest specific growth rate of 0.476 h⁻¹ was obtained for energy input of 525 J/m³. Higher microbial growth was seen for the cultures in the flasks sonicated for 20 min. The authors have explained their results on the basis of faster transport of the nutrients and oxygen across cell membrane, which reduced the lag period. On the other hand, larger lag time was seen at high ultrasound energy levels sufficient to induce cavitation. Jomdecha and Prateepasen⁴⁹ have suggested that cavitation and irradiation force from high ultrasonic energies could inactivate the microbial growth.

(5) Lanchun *et al.*⁵⁰ have reported the effect of low intensity ultrasound on physiological characteristics of *Saccharomyces cerevisiae*. The cells of *Saccharomyces cerevisiae* were grown at 29°C in YPD medium till the logarithmic growth phase was reached - after which the ultrasound treatment was applied at 24 kHz, 2 W power and 6.7% duty cycle (1 s sonication followed by 14 s silent treatment for every 15 s treatment). The characteristics of the ultrasound-treated cells such as flocculation, substrate consumption, ascospore production and proteinase activity were assessed. It was revealed that flocculation of the cells reduced after ultrasonic treatment. This result was attributed to alternations of the surface characteristics of the cell membrane induced by sonication. The substrate consumption rate increased with the sonication. Lanchun *et al.*⁵⁰ have attributed this result to change in membrane osmosis induced by sonication, in addition to boosting of the enzyme activity. On a whole, the cell metabolism was enhanced due to sonication. However, this enhancement was not permanent in nature, and was observed only in presence of ultrasound.

(6) Radel *et al.*⁵¹ studied the viability of *S. cerevisiae* cells (NCYC1006) in standing and propagating ultrasound wave field with frequency of 2.2 MHz and 14 W power. The standing wave field is created by interaction of the incident and reflected ultrasound wave from glass

surface of the flask holding the cell culture. For generation of the propagating wave field a spike-shaped sponge was attached to the glass surface of the flask so as to dampen and scatter the incident wave. In the standing wave field, the microbial cells are driven towards the pressure nodes due to Bjerknes forces and stay at this location. The viability of cells was determined using two methods: (i) measurement of the percentage of dead cells using methylene blue staining, and (ii) monitoring morphological changes under SEM. Micrographs of the sonicated yeast cells show morphological changes, as compared to the native cells. Ultrasound also altered the integrity of the cell vacuole, while the nucleus and the envelope of the cells are not affected. The presence of fermentation end products in the medium was found to influence separation and viability of the yeast cells. The loss of cell viability increased with concentrations of the end products in the medium, and leakage of intracellular material was also seen. Addition of 12% v/v ethanol in the medium disrupted the standing wave field. At these conditions the microbial cells were not concentrated at pressure nodes, but were dispersed in the medium. The agglomeration of yeast cells within the pressure nodal planes was revealed to minimise damaging effects of ultrasonic field on the cells.

(7) Schläfer *et al.*⁵² have studied improvement in the biological activity of microbial cultures in bioreactors at low ultrasound intensity. Microbial culture of *S. cerevisiae* was used with glucose as the substrate. Sonication treatment was carried out at 25 kHz frequency and two power levels, viz. 0.3 W/L for low energy ultrasound and 12 W/L for high power ultrasound. Interestingly, use of high power ultrasound did not yield higher ethanol. Schläfer *et al.*⁵² have claimed that due to low power, cavitation did not occur in the medium. However, sonication reduced the agglomeration of the cells. Intermittent sonication in the form of pulses resulted in greater production of ethanol as compared to continuous sonication. The microbial cells retained higher activity even after stoppage of sonication. Schläfer *et al.*⁵² have suggested enhancement in membrane permeability and the activity of the enzyme involved in intracellular metabolism as probable cause leading to enhancement in “bioactivity” of the microbial cultures, which is

manifested in higher bioethanol production.

(8) Wood *et al.*⁵³ have studied the enhancement effect of ultrasound on simultaneous saccharification and fermentation (SSF) process for ethanol production using mixed waste office paper as substrate. The mixed waste paper contained approximately 90% carbohydrate and 10% inert materials. *K. oxytoca* P2 was used as the microbial culture in fermentation. A mixture of two commercial enzymes, viz. Spezyme CP and Novozyme 188 was used for saccharification. Ultrasound was generated using a Telsonic 36 kHz tube resonator with maximum theoretical power of 150 W attached to the head plate of the fermenter. Enzyme stability (Cellulase and β -glucosidase) in presence of ultrasound treatment was ascertained. Control experiments with mechanical agitation revealed that kinetics of the saccharification process was limiting factor at the low enzyme concentrations. Sonication of the fermentation broth at 5.88% duty cycle (15 min sonication/240 min silent period) resulted in increased ethanol yield. For 24 h treatment, the ultrasound-induced enhancement in ethanol production was ~ 50% (ethanol concentration of 14.3 g/L against 9.5 g/L under control conditions), while for 96 h treatment the enhancement was ~ 15% (ethanol concentration of 34 g/L against 29.4 g/L under control conditions). This result indicated that influence of ultrasound on SSF process is more marked in terms of the kinetics rather than final yield of ethanol. It was revealed that sonication of the fermentation broth resulted in higher ethanol yield at relatively lower concentrations of the enzymes for hydrolysis. Intermittent sonication of the fermentation broth was more beneficial for saccharification than continuous sonication, which could decrease cellulase binding. Continuous sonication of the *K. oxytoca* microbial culture was found to inhibit sugar metabolism, cell growth and division. A probable cause underlying this effect could be leakage of intracellular metabolites and induction of SOS proteins. Intense microturbulence generated by ultrasound causes dissociation of the cellulose substrate that assists binding of the active enzymes at new sites for faster hydrolysis.

4. Mechanistic insight into ultrasound assisted synthesis of bioalcohols

The literature in the area of ultrasound assisted biomass pretreatment, enzymatic hydrolysis and fermentation reviewed in preceding sections have reported several beneficial influences of ultrasound irradiation or sonication on kinetics and yield of these processes. However, most of this literature is focused on results than rationale. Little attempt is dedicated in establishing the physical mechanism of the enhancement in kinetics or yield of the process induced by ultrasound and cavitation. In other words, the synergistic links between the physics/chemistry of the pretreatment, enzymatic hydrolysis and fermentation process and the physical/chemical effects of ultrasound and cavitation have not been explored and identified. In this section, we have presented a review of the literature that has investigated the pretreatment/hydrolysis/fermentation processes with mechanistic approach. In the papers reviewed in this section, an attempt is made to establish the physical mechanism of the influence of ultrasound and cavitation on the pretreatment/ hydrolysis/ fermentation systems by concurrent analysis of results of cavitation bubble dynamics simulations and the experimental results. These papers have also attempted to discriminate between the relative contribution of physical and chemical effects of ultrasound and cavitation to the enhancement.

4.1 Ultrasound assisted acid hydrolysis / alkaline delignification of biomass

As noted earlier, pretreatment of the biomass is an energy intensive step in the bioalcohol production. Combining conventional pretreatment techniques with sonication can enhance the kinetics/yield of the process with faster and higher production of reducible sugars. Rice is a major crop in many developing countries like India. The residues of rice crop (rice straw or rice husk) are rich in cellulose/hemicellulose, and hence, are potential fermentation substrates. Suresh *et al.*⁵⁴ have carried out mechanistic investigations of the sono-hybrid techniques for pretreatment of rice straw prior to fermentation to alcohol liquid fuels. Two chemical techniques *viz.* dilute acid and dilute alkali treatment, and two physical techniques *viz.* hot water bath and autoclaving were coupled with sonication. The yardstick for assessment of efficacy of sono-

hybrid techniques was total sugar and reducing sugar released. The total sugar release during acid and alkali pretreatment includes sugars in all forms, *viz.* monomer sugars (*i.e.* pentose sugars like xylose and arabinose, and hexose sugars like glucose and mannose), oligomers (cellobiose) and dehydrated forms that form at low pH from xylose and glucose like furfural and hydroxy methyl furfural. The reducing sugar or fermentable sugar fraction of total sugar essentially is the monomeric sugar. Suresh *et al.*⁵⁴ used the technique of application of elevated static pressure for discriminating between physical and chemical effects of ultrasound and cavitation. The experimental results were correlated with the simulations of cavitation bubble dynamics that predicted the magnitudes of micro-streaming, microturbulence and shock waves generated by ultrasound and cavitation. In addition, the acoustic streaming near the boundaries was also accounted for using the model of Nyborg⁵⁵ for steady circulations induced by high amplitude sound fields near surfaces of obstacles and vibrating elements and bounding walls. Nyborg⁵⁵ proposed that gas is released from solution under influence of ultrasound at solid-liquid surfaces, which leads to formation of gas nuclei on the surface. The oscillatory velocities of liquid induced by volume oscillations of these gas bodies generate highly localized streaming. As per analysis of Nyborg⁵⁵, the micro-streaming velocity induced by a pulsating hemispherical bubble has been determined as follows (Eq. 2):

$$U_{ms} = (U^2 / \omega R) \quad (2)$$

where U_{ms} is the velocity amplitude of oscillations of fluid elements, ω is the angular frequency of acoustic wave and R is the radius of the bubble. For acoustic pressure amplitude of 150 kPa, the velocity of fluid elements is 0.1 m/s. For an ultrasound frequency of 35 kHz as used by Suresh *et al.*⁸⁸ and 5 μm size bubble trapped in the biomass matrix, the localized micro-streaming velocity is 0.09 m/s.

Suresh *et al.*⁵⁴ observed following trends in release of reducing and total sugars:

(1) The physical technique of autoclaving alone did not give significant sugar release. However, coupled with sonication after autoclaving, the sugar release increased markedly.

(2) Sonication after autoclaving in acidic environment results in doubling of the sugar release. However, raising the static pressure of the system is revealed to reduce the sugar release.

(3) Highest sugar release (~ 54% w/w rice straw) was obtained for autoclaving, stirring followed by sonication in an acidic environment. As per the composition of rice straw, this was the highest possible sugar yield from rice straw with hydrolysis of all cellulose and hemicelluloses components of biomass.

The chemical mechanism of different reactions occurring during biomass pretreatment needs to be considered during analysis of the results. Autoclaving causes hydrolysis of hemicelluloses in biomass resulting in formation of organic acids like acetic acid. Water itself promotes hydrolysis at elevated temperatures due to change in ion product that assists in reaction of hemicelluloses. Autoclaving causes rapid thermal expansion of biomass, which opens up biomass structure with increased pore volume. Hot water bath treatment enhances cellulose digestibility and sugar extraction. Dilute acid treatment causes solubilization of hemicellulose fraction in biomass that leaves lignin and cellulose intact. This helps in increasing the accessibility of cellulose during enzymatic hydrolysis. High xylose (monosaccharide) yield with complete hydrolysis of oligomeric hemicelluloses saccharides can be obtained under optimized conditions of acid pretreatment. The main effect of alkaline pretreatment on biomass is delignification, but partial hydrolysis of hemicelluloses may also occur. Principal chemical mechanism of alkaline treatment is saponification of intermolecular ester bonds cross linking xylan hemicelluloses, other celluloses and lignin. Acetyl and uronic acid substitutions on hemicelluloses are removed during alkaline treatment. In addition to these chemical effects, alkaline treatment also has physical effects of swelling of biomass resulting in reduction in the degree of polymerization as well as crystallinity, increase in the surface area, disruption of lignin structure and the structural linkages between lignin and carbohydrates.

Above discussion clearly shows the role of mass transfer in the acid/alkali pretreatment of biomass. Long chain cellulose is less soluble in water than short chain oligomers formed as

intermediates during hydrolysis, but solubility of both reduces with temperature. Continuous liquid flow through the reaction system causes effective removal of the oligomers from the biomass matrix, which facilitates further dissolution of oligomers. This process increases the recovery of sugar monomers and oligomers, before they can degrade at the reaction conditions. This process also avoids re-precipitation of oligomers back onto surface of biomass due to less solubility at reduced temperature. Reactive lignin and sugar degradation products can promote reattachment of cellulose, hemicelluloses, their oligomers and lignin in the solution back to solid biomass, and these may also form complexes with monomeric sugars. Strong micro-convection generated ultrasound and cavitation cause effective circulation of water through biomass matrix with regular removal of monomeric sugars and refreshment of medium, which obviates these adverse effects. In addition to the physical effect of generation of intense microturbulence, radicals generated during transient collapse of cavitation bubbles can also enhance sugar release due to cleavage of lignin carbohydrate components.

(1) Increase in autoclaving period of biomass did not enhance sugar yield. The extent of hemicellulose hydrolysis may increase with higher periods of autoclaving. However, as the convection in the reaction system is low, sugar molecules are not effectively transported out of biomass matrix. Thus, sugar concentration in the bulk medium shows negligible change with increasing autoclaving periods. The autoclaving step followed by sonication of the reaction mixture helps effective transport of sugar molecules out of biomass matrix leading to increased sugar concentration in the bulk.

(2) Stirring of biomass solution after autoclaving also does not increase the sugar yield. The result of Suresh *et al.*⁵⁴ indicates that mechanical stirring of solution does not produce strong currents to penetrate biomass matrix leading to sugar transport out of biomass, as seen in case of sonication.

(3) Elevation of the static pressure of reaction system causes elimination of the transient cavitation events in the medium. However, only slight reduction in the sugar yield at elevated

pressure indicates negligible contribution of transient cavitation to the overall process of pretreatment and sugar release. Neither the microturbulence nor the shock waves generated by cavitation bubbles were intense enough to cause opening up of the biomass matrix and create liquid flow through the matrix that would assist sugar release. On the other hand, the contribution by micro-streaming due to ultrasound and acoustic streaming had greater contribution to enhancement of the transport of sugar molecules. The opening of biomass structure due to expansion is found to occur only with autoclaving (a thermal effect) and ultrasonic micro-streaming plays the secondary role of enhancing the transport of sugar molecules through the expanded biomass.

Ultrasound-assisted alkaline delignification: Singh *et al.*⁵⁶ have done mechanistic assessment of the process of alkaline delignification with ultrasound using waste biomass of *Parthenium hysterophorus*. NaOH was used as delignifying agent with pretreated biomass (after dilute acid hydrolysis + autoclaving) as substrate. The study included optimization of process parameters and conditions such as temperature, NaOH concentration and biomass concentration.

Extent of delignification under various conditions of treatment was done according to standard TAPPI⁵⁷ protocols. Characterization of delignified biomass was carried out using FTIR, XRD and FESEM analysis. Prior to analysis of experimental results, the chemical mechanism of delignification vis-à-vis the physical/chemical effects of ultrasound and cavitation needs to be considered:

Lignin is derived from three monomer units, *viz.* trans-coniferyl, trans-sinapyl and trans-*p*-coumaryl alcohol. These units are linked randomly mostly *via* ester linkages at α - and β - positions to construct the lignin macromolecules. The reactive sites in lignin are mainly the ester linkages and functional groups, since C-C are resistant to chemical attack. The areas of lignin susceptible to chemical attack are hydrolysable ester linkages, phenolic and aliphatic hydroxyl groups, methoxy groups, the unsaturated groups and uncondensed units. Main mechanism of lignin degradation in alkaline environment is the cleavage of α - and β - aryl ether

linkages. Ultrasound and cavitation can contribute to depolymerization and separation of lignin, in addition to degradation of lignin components. Fig. 1 shows the graphical simulations of radial motion of cavitation bubbles in alkaline solution of 1.5% w/v NaOH. It could be perceived that the temperature peak in the bubble at transient collapse reaches ~ 5000 K, at which the water molecules in the bubble dissociate forming $\cdot\text{H}$ and $\cdot\text{OH}$ radicals. The transient bubble collapse also generates acoustic waves of high pressure amplitude (~ 500 bar). Depolymerization of lignin with sonication can occur through homolytic cleavages of phenyl ether $\beta\text{-O-4}$ and $\alpha\text{-O-4}$ bonds, while separation of lignin due to sonication can occur as a result of cleavage of lignin–hemicellulose linkages. Lignin degradation may also be affected by hydroxyl radicals produced from transient cavitation bubbles. $\cdot\text{OH}$ radicals can attack aromatic ring leading to the formation of hydroxylated, demethoxylated and side chain eliminated products. A relatively small extent of attack can also occur on the side chain leading to the formation of dimers and oxidation of aromatic aldehydes to carboxylic acids. Increase in number of non–conjugated carboxyl moieties also indicates hydroxyl radical induced degradation. It should be noted that sonication can also cause lignin condensation and re–polymerization.

The major findings of Singh *et al.*⁵⁶ are as follows:

- (1) The kinetics of delignification is enhanced more than two fold with ultrasound.
 - (2) The extent of delignification with ultrasound was practically same in the range of 30–80°C.
- At higher biomass concentration, the extent of delignification reduced, while leveling–off of delignification was seen with respect to NaOH concentration above 2% w/v.

A mechanistic explanation to these results on the basis of bubble dynamic simulations can be given as follows: Although the intensity of transient cavitation reduces drastically with temperature, the intrinsic reactivity of OH^- increases, which compensates the effect, and thus delignification stays practically same in the temperature range of 30–80°C. Higher concentration of biomass causes scattering of the ultrasound waves, due to which intensity of convection in the system reduces. Strong convection generated by ultrasound and cavitation eliminates mass

transfer in the system making biomass accessible to OH^- ions. This leads to leveling off of delignification beyond certain concentration of NaOH.

XRD analysis revealed reduction in the crystallinity index of biomass after delignification, which is attributed to depolymerization of cellulose with ultrasound with scission of β -1-4 glycosidic bonds. FTIR spectra of delignified biomass revealed reduction in the intensities of all bonds corresponding to lignin removal, rupture of cellulose bonds and carbohydrate-lignin linkages. Moreover, the bond intensities corresponding to aromatic ring stretching and cellulose band also reduced. Changes in the XRD and FTIR spectra of biomass after delignification are essentially manifestations of the physical and chemical effects of cavitation. Reduction in aromatic ring stretching and aromatic ring vibration bonds along with reduction in bonds corresponding to side chain removal are attributed to reactions induced by $\cdot\text{OH}$ radicals from transient cavitation. Transient cavitation also generates high pressure amplitude shock waves. The biomass particles get drifted randomly in these waves at high velocities leading to collision between them. The energy released in such collisions is sufficient to cause hemolytic cleavage of phenyl esters β -1-4 and α -1-4 bonds leading to depolymerization of lignin. FESEM micrographs depicted in Fig. 2 reveal higher surface roughness for biomass delignified with sonication (as a result of erosion or attrition induced by strong microconvection), as compared to the biomass treated with mechanical agitation. Thus, the study of Singh *et al.*⁵⁶ portrays a vivid picture of mechanistic facets of ultrasonic delignification.

4.2 Ultrasound assisted enzymatic hydrolysis

Bharadwaja *et al.*³² has made a preliminary assessment of the effect of ultrasound on enzymatic hydrolysis of delignified biomass. Two commercial enzymes, *viz.* cellulase and cellobiase, were employed for hydrolysis. Initially, statistical optimization of the enzymatic hydrolysis with mechanical shaking was carried out using Central Composite Design (CCD) coupled with Response Surface Method (RSM) analysis for the optimization parameters of the

concentrations of the two enzymes and the biomass concentration. Later, for the optimum conditions of mechanical shaking, sonication was applied. However, the temperature of reaction mixture was reduced to 30°C for sonication (against 50°C for mechanical shaking), as the intensity of transient bubble collapse and the associated physical/chemical effects reduce with temperature. The kinetics of enzymatic hydrolysis was found to increase 18-fold with ultrasound. Analysis of experimental results with Michaelis–Menten Model and Lineweaver–Burk plots revealed that values of V_{\max} (reaction velocity) increased 18-fold while values of K_m (substrate affinity constant) remained constant when mechanical shaking was replaced with sonication. Bharadwaja *et al.*³² attributed to enhancement in reaction velocity to enhancement in convection in the medium that eliminates mass transfer, and increases the accessibility of substrate for the enzyme. The enzyme–substrate affinity, however, is an intrinsic property, which does not show any beneficial influence of ultrasound. The findings of Bharadwaja *et al.*³² gave a preliminary insight into the influence of ultrasound on enzymatic hydrolysis of biomass. The matter of ultrasound-assisted enzymatic hydrolysis has been later dealt with in greater detail and rigor by Borah *et al.*⁵⁸, whose findings are summarized later in this section. Bharadwaja *et al.*³² have developed a complete conceptual process for bioethanol production from *P. hysterophorus*, which includes all three steps of biomass pretreatment and fermentation of both pentose and hexose hydrolyzates obtained from dilute acid pretreatment and enzymatic hydrolysis. The flow sheet for this conceptual process with complete mass balance is shown in Fig. 3. It could be inferred from Fig. 3 that the total bioethanol yield from *P. hysterophorus* is 256 g/kg of raw biomass.

Singh *et al.*⁵⁹ have investigated the mechanics of ultrasound assisted enzymatic hydrolysis of pretreated and delignified biomass of *Parthenium hysterophorus*. This study comprised of two parts, viz. 1. optimization of the enzymatic hydrolysis using statistical design of experiments using mechanical agitation, and 2. intensification of enzymatic hydrolysis with ultrasound at optimized conditions. The experimental results were fitted to the first-order

product-inhibited HCH-1 model for enzymatic hydrolysis of cellulose.^{60, 61} The reaction mechanism for this model is shown in Fig. 4A, while the schematic of the mechanism of ultrasound-assisted enzymatic biomass hydrolysis is depicted in Fig. 4B. A brief description of this model is as follows.⁵⁹ This model hypothesis that first step in enzymatic hydrolysis of cellulose is adsorption of free cellulose, E^f , on to free site cellulose, G_x^f . This adsorption is reversible. Combination of active site of adsorbed enzyme with cellulose site yields enzyme/substrate complex, characterized by the equilibrium constant, $1/\eta$. Irreversible decomposition of the enzyme/substrate complex yields the solute product, G_s . The rate constant of the hydrolysis step is given by k . HCH-1 model also hypothesis that enzyme in all forms (free, adsorbed and complex) can be inhibited by the product (glucose), which is characterized by product binding constant, β . The net reaction velocity is given as:

$$v = \frac{\kappa[G_x][E] \left(\frac{1}{1 + \beta[G_s]} \right)}{\alpha + \phi[G_x] + \varepsilon[E]} \quad (3)$$

where $\kappa = \frac{k}{\eta + 1}$, $\alpha = \frac{\eta\varepsilon}{\eta + 1}$ and factor ϕ signifies extent of enzyme adsorption onto cellulose,

and is given as:

$$\phi = \frac{\alpha}{\alpha + \varepsilon(1 + \beta[G_s])[E^f]} \quad (4)$$

The four parameters, viz. α , β , ε and κ , in the expression for reaction velocity characterize the kinetics and physiology of the enzymatic hydrolysis process. Singh *et al.*⁵⁹ have matched the numerical solution of the ordinary differential equation for reaction velocity with experimental profile of total reducing sugar using Genetic Algorithm. This match essentially yields the optimum values of the four parameters listed above, which gives physical insight into ultrasound assisted enzymatic hydrolysis. The major findings and conclusions of Singh *et al.*⁵⁹ are summarized below:

(1) The results of Lineweaver-Burk analysis, i.e. the values of Michaelis-Menten model parameters K_m and V_{max} revealed that sonication not only increases enzymatic/substrate affinity (indicated by reduction in K_m), but also enhances conversion of enzyme/substrate complex into products as indicated by increase in reaction velocity, V_{max} . Reduction in K_m is attributed to enhanced convection and mass transfer, resulting in greater interaction of enzyme and substrate. This is essentially a consequence of micro-turbulence and intense micro-mixing generated by ultrasound and cavitation in reaction mixture. Increase in V_{max} (due to faster splitting of enzyme-substrate complex and diffusion of solute products into bulk) is also attributed to enhanced convection due to ultrasound/cavitation.

(2) As noted earlier, matching of the experimental and simulated time profiles of total reducing sugar yield in enzymatic hydrolysis through Genetic Algorithm optimization yields the values of kinetic/physiological parameters of the HCH-1 model, which are listed in Table 4. Comparative evaluation of the parameters of HCH-1 model under control (mechanical agitation) and test (sonication) conditions reveals following trends that demonstrates the effect of sonication on enzymatic hydrolysis: 1. Increase in lumped kinetic constant (κ) of hydrolysis; 2. Reduction in lumped constant of enzyme/ substrate complexation (α); 3. Reduction in the product binding constant (β) indicative of level of product inhibition; and 4. No change in extent of enzyme adsorption on cellulose site. A physical explanation for these results can be given as follows: Enhancement in κ and α can be explained along same lines as the trends in Lineweaver-Burk parameters (K_m and V_{max}) stated previously. Reduction in product binding constant is essentially an outcome of the faster transport of the product of enzyme hydrolysis (i.e. glucose) away from biomass and further dilution in the reduction due to intense micro-mixing. Rapid transport of glucose away from cellulose surface and dilution in the medium reduces the probability of binding of product to the active sites of enzyme resulting in inhibition. Similar values of ϕ in control and test experiments point out that mass transfer is not a limiting factor for enzyme

adsorption on cellulose. The net effect of the variation in κ , α and β with sonication is 4-fold increase in kinetics of enzyme hydrolysis with sonication, although the net sugar yield shows only a marginal improvement of $\sim 20\%$. Singh *et al.*⁵⁹ have hypothesized that ultrasound-induced enhancement of the kinetics of enzyme hydrolysis could be a consequence of “unfolding” of the proteins of enzymes, cellulase and β -glucosidase. Intense mass turbulence generated by ultrasound and cavitation could induce conformational changes in the secondary structure of enzymes, which results in exposure of the inner hydrophobic amino acid residues that increase the activity of the enzyme. This hypothesis has later been confirmed by Borah *et al.*⁵⁸ as explained in detail later in this section.

Borah *et al.*⁵⁸ have investigated the ultrasound-induced enhancement of enzymatic hydrolysis of invasive biomass species. Pretreated and delignified biomasses of four invasive weeds, viz. *S. spontaneum*, *M. micrantha*, *L. camara* and *E. crassipes* were subjected to enzymatic hydrolysis under mechanical agitation or mechanical agitation coupled with sonication. The study of Borah *et al.*⁵⁸ also included assessment of the morphological changes in the secondary and tertiary structures of the cellulase and cellobiase enzyme induced by physical/chemical effects of ultrasound/cavitation. This assessment has been done using intrinsic fluorescence and circular dichroism analysis. The circular dichroism spectra of native and ultrasound treated cellulase and cellobiase enzymes were analyzed using DICHROWEB server.⁶²⁻⁶⁴

The intrinsic fluorescence spectra and circular dichroism spectra of the cellulase and cellobiase enzyme are shown in Figs. 5 and 6, respectively. Mainly three amino acid residues (viz. Trp, Tyr and Phe) contribute to intrinsic fluorescence. Fig. 5 shows the Trp fluorescence spectrum for cellulase and cellobiase enzymes individually, and also for their mixtures, with maximum fluorescence emission wavelength at 348 nm. Although enzymatic treatment with mechanical agitation and sonication causes reduction in fluorescence intensity, this effect is more marked for sonication. The fluorescence spectra do not show any red or blue shift in

optimum fluorescence emission wavelength, which is a consequence of rupture of hydrophobic interaction between protein molecules leading to molecular unfolding of proteins. This is attributed to intense micro-convection generated by ultrasound and cavitation. These conformational changes cause exposure of hydrophobic amino-acid groups and structures inside enzyme molecules, which results in augmentation of the enzyme activity. The structural analysis of the CD spectra of cellulase and cellobiase enzymes and their mixtures (shown in Fig. 6) further corroborate the results of fluorescence spectroscopy. Percentage contents of the secondary structure components of the enzymes are depicted in Table 5A. The data shown in Table 5A clearly showed reduction in α -helix conformation content of the enzyme, with rise in β -sheet and random coil structure. Reduction in α -helix content of both enzymes is more marked for ultrasound treatment than mechanical agitation. These conformational changes help in augmenting the activities of both cellulase and cellobiase enzymes. As per analysis of Davies and Henrissat⁶⁵ and Rouvinen *et al.*⁶⁶, the active sites of cellulase and cellobiase enzymes are located in the β -barrel tunnels, and increase in β -sheet/ β -turn components in enzyme structure can increase the number of active sites enhancing the enzyme activity. Moreover, reduction in α -helix components can also expose catalytic sites inside located them, due to which the substrate can bind to the enzyme more easily—without requiring undergoing twisted and linear confirmations. These effects can also result in augmentation of catalytic efficiency of the enzyme.

Borah *et al.*⁵⁸ have fitted the experimental profiles of reducing sugar concentration during enzymatic hydrolysis of the invasive weeds under control (mechanical agitation) and test (sonication) to the HCH-1 model described earlier. Table 5B depicts the principal results of study of Borah *et al.*⁵⁸. Sonication enhanced the kinetics of the enzymatic hydrolysis by more than 10-fold, in that nearly same TRS yield was obtained with sonication in 10 h treatment as against 120 h treatment with mechanical agitation. The parameters of the HCH-1 model viz. κ , α , β and ε for control (mechanical agitation) and test (sonication) conditions shows following

trend; which reveals the mechanism of the effect of sonication on enzymatic hydrolysis: (1) enhancement of lumped kinetic constant (κ) of the hydrolysis; (2) reduction in lumped constant for enzyme/ substrate complexation (α); (3) reduction in product binding constant (β), and (4) similar values of ε under test (sonication) and control (mechanical agitation) conditions. These trends are quite similar to those observed in the study of Singh *et al.*⁵⁹ for the enzymatic hydrolysis of *Parthenium hysterophorus*. Explanation for these trends can be given along similar lines as in study of Singh *et al.*⁵⁹: Enhancement in κ , with concurrent reduction in α is attributed to micro-turbulence and intense micro-mixing generated by ultrasound/cavitation in the reaction mixture, which promotes faster transport and enhanced interaction of enzyme with substrate. Intense micro-convection also helps in faster diffusion of the soluble product away from cellulose surface and its dilution in the medium. This reduces the extent of product inhibition by enzyme, as indicated by reduction in β . Intense micro-turbulence also assists faster splitting of the enzyme-substrate complex, which results in enhanced reaction velocity—as indicated by larger value of lumped kinetic constant κ . A practically same value of ε with mechanical agitation and sonication point out that enzyme adsorption on cellulose is not limited by mass transfer.

A peculiar feature of the study of Borah *et al.*⁵⁸ was that conditions of enzyme hydrolysis (such as pH, temperature, substrate concentration and enzyme concentration) were not optimized for the biomasses of each of four invasive weed. The enzyme hydrolysis was carried out for the same conditions as that for hydrolysis of *Parthenium hysterophorus* (in the study of Singh *et al.*⁵⁶). Despite non-optimum conditions, the enhancement effect of sonication (in terms of several fold rise in hydrolysis kinetics) was observed. This result essentially points out that process intensification due to ultrasound/ cavitation helps in overcoming the limitation of non-optimum conditions during enzymatic hydrolysis. The study of Borah *et al.*⁵⁸ has thus provided deeper mechanistic insight into the enhancement of enzymatic hydrolysis due to sonication.

4.3 Ultrasound assisted ethanol fermentation: Separate Hydrolysis and Fermentation (SHF) mode

Singh *et al.*⁶⁷ have presented mechanistic investigations in ultrasound-assisted bioethanol fermentation using *Parthenium hysterophorus* biomass. Ultrasound of 35 kHz frequency and 1.5 bar pressure amplitude with 10% duty cycle was employed. The protocol for experiments was separate hydrolysis and fermentation (SHF). Both steps of enzymatic hydrolysis and fermentation have been carried out with sonication. The experimental profiles of concentration of total reducing sugar, cell mass and ethanol during fermentation were fitted to the mathematical model proposed by Philippidis *et al.*⁶⁸, which is based on the HCH-1 model of Holtzapfle⁶⁰ and Holtzapfle *et al.*⁶¹. The essential equations of this model are as follows:

Cell mass: Glucose is assumed to be the primary carbon source, which is metabolized into cell mass, with concomitant synthesis of ethanol and CO₂. The microbial (or cell mass) growth as a function of glucose and ethanol concentration has been described using a Monod type kinetic expression, which includes non-competitive substrate inhibition and non-competitive product inhibition, as follows:

$$\frac{dX}{dt} = \mu_m \left[\frac{G}{K_3 + G + G^2/K_i} \right] \left[\frac{K_{3E}}{K_{3E} + E} \right] X - k_d X \quad (5)$$

Glucose: The glucose in fermentation broth is consumed through cell mass synthesis and cell maintenance requirement. The profile for glucose is given as:

$$\frac{dG}{dt} = - \left[\frac{1}{Y_{X/G}} \frac{dX}{dt} + m(X) \right] \quad (6)$$

Ethanol: Ethanol is formed through two mechanisms, viz. growth-associated and non-growth associated, and it is also a function of glucose concentration in the medium as follows:

$$\frac{dE}{dt} = \left[a \left(\frac{dX}{dt} \right) + b(X) \right] \left[\frac{G}{K_4 + G} \right] \quad (7)$$

The set of three differential equations in the Philippidis model and the kinetic/ physiological

parameter therein characterize the fermentation process. The three equation for X , G and E have total 10 parameters, viz. K_3 , K_i , K_{3E} , k_d , μ_m , a , b , $Y_{X/G}$, m and K_4 . Fitting of this model to experimental profiles of X , G and E yields the numerical values of the parameters in the model. Comparative analysis of the model parameters under control (mechanical agitation) and test (sonication) conditions give physical insight into the influence of ultrasound / cavitation on fermentation process.

Principal findings of the experimental and modeling studies of Singh *et al.*⁶⁷ were as follows: (1) As compared to the control experiments (with mechanical agitation), the test experiments (with sonication) had 2-fold higher productivity. Moreover, the final ethanol and cell mass concentration attained with sonication was 10% higher as compared to mechanical agitation. (2) Experimental and simulated profiles of cell mass, glucose and ethanol concentration showed good match indicating suitability of Philippidis model. The model parameters showed following trends under test and control conditions:

- a. Reduction in Monod constant for glucose for cell growth (K_3), which reveals higher utilization of substrate for cell growth.
- b. Increase in inhibition constant (K_i) for cell growth, which points at higher tolerance of the cells towards non-competitive substrate inhibition.
- c. Enhancement in maximum specific growth rate, with concurrent reduction in specific death rate in test conditions.
- d. Similar values of K_{3E} for test and control conditions, which reveals that inhibition of cell growth by product (ethanol) is unaltered with sonication.

These trends in the model parameters are essentially manifestations of the physical/chemical effects of ultrasound and cavitation. Reduction in Monod constant for cell growth (which is substrate concentration required to achieve half of maximum specific growth rate of biomass) essentially represents faster transport of glucose across cell membrane due to which lesser bulk concentration of glucose is required to achieve maximum specific growth rate.

Sonication also assisted better utilization of glucose for cell growth, which is endorsed by increase in values of $Y_{X/G}$ and μ_{\max} . Faster transport and utilization of glucose also resulted in rise in inhibition constant, K_i , which indicates cells' better tolerance towards substrate inhibition. Concurrent reduction in K_3 and rise in K_i could be considered as synergistic effects of sonication on fermentation. Similar values of K_{3E} (inhibition constant for product ethanol) for both control and test experiments indicates that this is an intrinsic physiological property of the cells, which does not depend on the ambience (or environment) of the cells. Ethanol is essentially a growth associated product (associated with energy generation by microorganism). Nevertheless, the non-zero value for the constant b in equation 7, indicated that ethanol fermentation also occurred during stationary phase, which is non-growth associated production. Moreover, similar values of constants a and b for control and test experiments show that these are also intrinsic properties, which do not depend on the ambience of cell.

The values of k_d (specific cell death rate) and m (specific substrate consumption rate for cell maintenance) also reduced under sonication. Cellular maintenance represents energy expenditure for repair of damaged cellular components and transfer of nutrients and products across cell membrane. It also includes the energy required for motility and for adjustment of osmolality of the cells interior volume. The intense micro-mixing and micro-convection generated by ultrasound waves assists cell motility, de-agglomeration of the cells and trans-membrane transport, which helps in regulation of osmolality. An implication of this is reduction in cells' dependence on substrate for maintenance and utilization of large fraction of glucose ethanol production. Depletion of nutrients and accumulation of toxic products is the principal cause leading to death phase of cells. The intense micro-turbulence generated by ultrasound/cavitation results in efficient transfer of nutrient across cells. Moreover, it also assists transport of toxic substances away from the cells with their dilution in the medium. Both of these effects lead to enhancement of growth phase with simultaneous reduction in cell death rate. Similar value of K_{3E} in test and control experiments can be explained as follows: Thomas and Rose⁶⁹

and Leao and van Uden⁷⁰ have attributed inhibition of cell growth to reduction in fluidity of plasma membrane due to inhibitory effect of ethanol on action of proteins involved in transport of compounds in the cells. Secondly, modification of lipid content in the environment of the sugar transport system by ethanol also has major effect on membrane permeability. These mechanisms are mainly of intrinsic type and remain unaffected by physical effect of microturbulence/ microconvection induced by ultrasound/ cavitation. Thus, values of K_{3E} for test and control experiment are similar.

Singh *et al.*⁶⁷ have also assessed the effect of sonication on morphology and viability of yeast cells using flow cytometric analysis. No change in SSC and FSC was observed after sonication of the microbial cells, which indicated that internal complexity and morphology of yeast cells remained intact during sonication with no adverse effect.

4.4 Ultrasound assisted ethanol fermentation: Simultaneous Saccharification and Fermentation (SSF) mode

In another study, Singh *et al.*⁷¹ have explored the physical mechanism of influence of ultrasound on fermentation of pretreated and delignified biomass of *Parthenium hysterophorus* for ethanol production in the SSF (simultaneous saccharification and fermentation) mode. The fermentation model of Philippidis *et al.*⁶⁸ described earlier was used for fitting of experimental results. However, due to experimental limitations for estimation of profiles of cellulose and intermediate dimeric cellobiose, only the equations for cell mass and ethanol concentration in the Philippidis model were used for fitting of the experimental data. These equations had a total of 7 parameters, viz. K_3 , K_i , K_{3E} , k_d , μ_m , a and b ; values of which were obtained after matching experimental and simulated profiles using Genetic Algorithm. These results have been correlated with the simulations of cavitation bubble dynamics using diffusion limited model of Toegel.⁷² Table 6 depicts the kinetic and physiological parameters in the fermentation model, while Table 7 depicts the summary of cavitation bubble dynamics simulations, i.e. the physical and chemical effects of transient cavitation. The main results and analysis of Singh *et al.*⁷¹ is summarized

below:

1. The most notable effect of sonication on SSF process was 3-fold reduction in time of fermentation. A marked 4-fold increase in productivities of ethanol and cell mass concentration was achieved with sonication, as compared to mechanical agitation. The final ethanol titre was 15.62 g/L with yield of 0.4 g ethanol/g pretreated biomass or 0.21 g ethanol/ g raw biomass.
2. Comparative analysis of the physiological parameters of the fermentation model under control (mechanical agitation) and test (sonication) conditions revealed following mechanistic account of the influence of ultrasound/ cavitation on the SSF process, which has significant similarity to the SHF process: (a) Reduction in K_3 , Monod constant for glucose for cell growth. (b) Increase in maximal specific growth rate (μ_m) and reduction in specific cell death rate. (c) Rise in K_i , inhibition constant of cell growth by glucose, indicating increased tolerance of cells towards non-competitive inhibition by substrate. Similar to SHF process, concurrent reduction in K_3 and K_i is a synergistic effect attributed to faster transport and utilization of glucose due to intense mixing generated by ultrasound/ cavitation. (d) Similar values of K_{3E} (inhibition constant of cell growth by ethanol) in control and test experiments - indicating sole dependence of this property on the physiological of the cells and not on their ambience. (e) As stated earlier, ethanol production by cells is a growth-associated process and is related to energy generation by microorganisms. However, the parameter b in equation 13, has a non-zero value of 1.99 g/g/h, which implies that ethanol production also occurs in stationary phase of cell life cycle. However, larger numerical value for parameter a than b signifies that ethanol production is predominantly a growth-associated process.

Along similar lines as for the SHF process of fermentation, an explanation for these results can be given as follows: There are two causes leading to cell growth inhibition by ethanol, viz. (1) inhibition of enzymes involved in the glycolytic pathway, and (2) effects on fluidity, transport mechanism or enzymes associated with membrane (as noted earlier). As these properties are mostly of intrinsic type, they are not affected by the physical or chemical effects

of ultrasound/ cavitation. Another peculiar feature of the study of Singh *et al.*⁷¹ was that despite use of low activity cellulase enzyme (for hydrolysis of cellulose) from natural isolates, the net productivity and yield of ethanol was at par with the studies using commercial enzymes. This result is also attributed to the enhancement effect induced by microconvection generated by ultrasound/ cavitation, due to which the activities of cruder enzymes are improved.

A comparative analysis of the two studies by Singh *et al.*^{67, 71} employing SHF and SSF protocols gives interesting accounts of links between physical effects of sonication and mode of fermentation. Higher values of maximum ethanol concentration in ultrasound-assisted fermentation in SSF mode (as compared to SHF mode) is attributed to acceleration of fermentation as well as enzymatic hydrolysis under the influence of ultrasound. However, the ethanol productivity in SHF mode is higher than SSF. This could lead to misinterpretation that SHF process is more efficient than SSF. However, it should be noted that the productivity in the SHF protocol has been determined only on the fermentation period (which does not include the time for enzymatic hydrolysis). The cell mass concentration in SHF and SSF mode shows inverse trend in that SSF mode achieves higher cell concentration. An explanation for this result is given along following lines: intense micro-convection due to ultrasound/ cavitation in SSF protocol causes significant augmentation of the rate of enzymatic hydrolysis. This can significantly enhance the instantaneous levels of sugar concentration in the fermentation broth - even higher than those achieved in SHF mode, which leads to higher cell mass production. Fermentation in SHF protocol starts with highest concentration of reducing sugar, which continuously reduces with time. On the other hand, in SSF protocol, the enzymatic hydrolysis of solid cellulose occurs simultaneously with the fermentation, which results in continuous generation of reducing sugar in the broth. Therefore, the time – averaged concentration of reducing sugar in the broth in SSF protocol is likely to be higher than the SHF protocol, which is manifested in terms of larger cell mass concentration. Comparing the cell mass concentration under control conditions (mechanical agitation) in SHF and SSF protocol, an opposite trend is

seen in that SSF protocol yields lesser cell mass. This is attributed to slower kinetics of the enzymatic hydrolysis using mechanical agitation due to which the time-averaged sugar concentration in the fermentation broth is expected to be lesser than the SHF protocol.

6. Overview and conclusions

Bioalcohols have emerged as potential renewable alternate liquid transportation fuels. However, large scale production of bioalcohols has been hampered by factors like uneconomic cost of conventional substrates and slow kinetics of enzymatic hydrolysis and fermentation. Use of cheap substrates such as lignocellulosic biomass is a viable solution; however, the energy intensive step of biomass pretreatment adds to the production cost. New technologies employing smart ways of introducing energy into the system can improve the kinetics/ yield of the bioalcohol production process, which can boost their economy. Sonication (or ultrasound irradiation) is one such technology. Laboratory scale studies on ultrasound-assisted biomass pretreatment, enzymatic hydrolysis and fermentation have given encouraging results. In order to successfully scale up ultrasound-assisted bioalcohol processes, knowledge of the physical mechanism of the process linking the physics/chemistry of the process, and the physical/chemical effects of ultrasound and cavitation is necessary. In this review, we have attempted to present a critical analysis of the literature in the area of ultrasound assisted biomass pretreatment and fermentation. This review also includes critical analysis of the literature that has investigated the mechanistic issues of ultrasound assisted processes. The analysis of results of published literature essentially points at physical effects of ultrasound and cavitation to be beneficial towards intensification of various steps in bioalcohol production process. Intense microconvection and microturbulence generated by ultrasound and cavitation enhance the transport characteristics of the biomass pretreatment and fermentation system. Microconvection also assists in enhancing activity of the enzymes and microbial cells, which boosts the yield/kinetics of the enzymatic hydrolysis and fermentation. It also helps in reduction of

substrate/product inhibition and assists faster growth of microbial culture itself.

To summarize: ultrasound-assisted bioalcohol production (including biomass pretreatment and fermentation) has high potential for commercialization, but also has highly interwoven physics and chemistry. Proper investigations from mechanistic view point are crucially important for efficient optimization and scale up of the process. This review is likely to be a useful source of literature in the area of ultrasound-assisted biomass pretreatment, enzymatic hydrolysis and fermentation, and its critical mechanistic analysis for the scientific fraternity in bioalcohol synthesis.

Supplementary Material

The following information has been provided as supplementary material with this paper: Section entitled Physics of ultrasound and cavitation: A brief overview, along with two tables, viz. Table S.1: Essential equations (ODE's) of the diffusion-limited ODE model, and Table S.2: Thermodynamic data for the diffusion limited model

Acknowledgments

Authors gratefully acknowledge the anonymous reviewers for their meticulous assessment of the manuscript and constructive criticism.

References

- 1 A. Ranjan and V. S. Moholkar, *Int. J. Energy Res.*, 2012, 36(3), 277–323.
- 2 K. S. Suslick, *Science*, 1990, 247, 1439–1445.
- 3 E. J. Hart and A. Henglein, *J. Phys. Chem.*, 1985, 89(20), 4342–4347.
- 4 E. J. Hart and A. Henglein, *J. Phys. Chem.*, 1987, 91, 3654–3656.
- 5 J. Luo, Z. Fang and Jr. R. L. Smith, *Prog. Energ. Combust. Sci.*, 2014, 41, 56–93.
- 6 V. S. Moholkar, H. A. Choudhury, S. Singh, S. Khanna, A. Ranjan, S. Chakma

and J. B. Bhasarkar, in *Production of Biofuels and Chemical with Ultrasound, Biofuels and Biorefineries series* (Vol. 4), eds Z. Fang, R. L. Smith and X. Qi, Springer Science + Business Media, Dordrecht, 2015, Physical and chemical mechanisms of ultrasound in biofuel synthesis, 35–86.

7 P. Kumar, D. M. Barrett, M. J. Deelwiche and P. Stroeve, *Ind. Eng. Chem. Res.*, 2009, 48(8), 3713–3729.

8 V. Menon and M. Rao, *Prog. Energy Combust. Sci.*, 2012, 38(4), 522–550.

9 M. R. Esfahani and M. Azin, *Asia–Pac. J. Chem. Eng.*, 2012, 7, 274–278.

10 M. Kunaver, E. Jasiukaitytė and N. Čuk, *Bioresour. Technol.*, 2012, 103, 360–366.

11 D. J. Pejin, L. V. Mojovic, J. D. Pejin, O. S. Grujic, S. L. Markov, S. B. Nikolić and M. N. Markovic, *J. Chem. Technol. Biotechnol.*, 2012, 87, 170–176.

12 A. García, M. G. Alriols, R. Llano–Ponte and J. Labidi, *Bioresour. Technol.*, 2011, 102, 6326–6330.

13 M. Y. Harun, A. B. D. Radiah, Z. Z. Abidin and R. Yunus, *Bioresour. Technol.*, 2011, 102, 5193–5199.

14 S. Nikolić, L. Mojović, M. Rakin, D. Pejin and J. Pejin, *Clean Techn. Environ. Policy*, 2011, 13, 587–594.

15 B. Karki, B. P. Lamsal, S. Jung, J. van Leeuwen, A. L. Pometto III, D. Grewell and S. K. Khanal, *J. Food Eng.*, 2010, 96, 270–278.

16 S. Nikolić, L. Mojović, M. Rakin, D. Pejin D and J. Pejin, *Food Chem.*, 2010, 122, 216–222.

17 R. Yunus, S. F. Salleh, N. Abdullah and D. R. A. Biak, *Bioresour. Technol.*, 2010, 101, 9792–9796.

18 S. Nitayavardhana, S. K. Rakshit, D. Grewell, J. van Leeuwen and S. K. Khanal, *Biotechnol. Bioeng.*, 2008, 101, 487–496.

- 19 T. Aimin, Z. Hongwei, C. Gang, X. Guohui and L. Wenzhi, *Ultrason. Sonochem.*, 2005, 12, 467–472.
- 20 M. J. Bussemaker, F. Xu and D. Zhang, *Bioresour. Technol.*, 2013, 148, 15–23.
- 21 P.B. Baxi and A. B. Pandit, *Bioresour. Technol.*, 2012, 110, 697–700.
- 22 S. Sasmal, V. V. Goud and K. Mohanty, *Energy Fuels*, 2012, 26, 3777–3784.
- 23 R. Velmurugan and K. Muthukumar, *Biochem. Eng. J.*, 2012a, 63, 1–9.
- 24 R. Velmurugan and K. Muthukumar, *Bioresour. Technol.*, 2012b, 112, 293–299.
- 25 W. Chen, H. Yu, Y. Liu, P. Chen, M. Zhang and Y. Hai, *Carbohy. Polym.*, 2011, 83, 1804–1811.
- 26 R. Velmurugan and K. Muthukumar, *Bioresour. Technol.*, 2011, 102, 7119–123.
- 27 T.–Q. Yuan, F. Xu, J. He and R.–C. Sun, *Biotechnol. Adv.*, 2010, 28, 583–593.
- 28 Y. Zhang, E. Fu and J. Liang, *Chem. Eng. Technol.*, 2008, 31:1510–1515.
- 29 J.–X. Sun, R. Sun, X.–F. Sun, Y. Su, *Carbohyd Res.* 2004, 339, 291–300.
- 30 R. C. Sun, X. F Sun and X. H. Ma, *Ultrason. Sonochem.*, 2002, 9, 95–101.
- 31 R. C. Sun and J. Tomkinson, *Ultrason. Sonochem.*, 2002, 9:85–93.
- 32 S. T. P. Bharadwaja, S. Singh and V. S. Moholkar, *J. Taiwan Inst. Chem. Eng.*, 2015, 51, 71–78.
- 33 A. Z. Sulaiman, A. Ajit, R. M. Yunus and Y. Chisti, *Biotechnol. Prog.*, 2013, 29(6), 1448–1457.
- 34 Q. Li, G. –S. Ji, Y. –B. Tang, X.–D. Gu, J.–J. Fei and H.–Q. Jiang, *Bioresour. Technol.*, 2012, 107, 251–257.
- 35 K. Ninomiya, K. Kamide, K. Takahashi, N. Shimizu, *Bioresour. Technol.*, 2012, 103, 259–265.
- 36 B. Karki, D.Maurer and S. Jung, *Bioresour. Technol.*, 2011, 102, 6522–6528.
- 37 M. Montalbo–Lomboy, L. Johnson, S. K. Khanal, J. van Leeuwene and D. Grewell, *Bioresour. Technol.*, 2010, 101, 351–358.

- 38 F. Yang, L. Li, Q. Li, W. Tan, W. Liu and M. Xian, *Carbohydr. Polym.*, 2010, 81, 311–316.
- 39 S. D. Shewale and A. B. Pandit, *Carbohydr. Res.*, 2009, 344, 52–60.
- 40 J. Yu, J. Zhang, J. He, Z. Liu and Z. Yu, *Bioresour. Technol.*, 2009, 100, 903–908.
- 41 S. K. Khanal, M. Montalbo, J. van Leeuwen, G. Srinivasan and D. Grewell, *Biotechnol. Bioeng.*, 2007, 98, 978–985.
- 42 C. Z. Li, M. Yoshimoto, H. Ogata, N. Tsukuda, K. Fukunaga and K. Nakao, *Ultrason. Sonochem.*, 2005, 12, 373–384.
- 43 M. Imai, K. Ikari and I. Suzuki, *Biochem. Eng. J.*, 2004, 17, 79–83.
- 44 C. Li, M. Yoshimoto, N. Tsukuda, K. Fukunaga and K. Nakao, *Biochem. Eng. J.*, 2004, 19, 155–164.
- 45 T. Sivasankar, A. W. Paunikar and V. S. Moholkar, *AIChE J.*, 2007, 53, 1132–1143.
- 46 C. Ofori–Boateng and K. T. Lee, *Fuel*, 2014, 119, 285–291.
- 47 P. Indra Neel, A. Gedanken, R. Schwarz and E. Sendersky, *Energy Fuels*, 2012, 26, 2352–2356.
- 48 A.Z. Sulaiman, A. Ajit, R. M. Yunus and Y. Chisti, *Biochem. Eng. J.*, 2011, 54:141–150.
- 49 C. Jomedcha and A. Prateepasen, *Lett. Appl. Microbiol.*, 2010, 52, 62–69.
- 50 S. Lanchun, W. Bochu, Z. Liancai, L. Jie, Y. Yanhong and D. Chuanren, *Colloids Surf. B*, 2003, 30, 61–66.
- 51 S. Radel, A. J. McLoughlin, L. Gherardini, O. Doblhoff–Dier and E. Benes, *Ultrasonics*, 2000, 38, 633–637.
- 52 O. Schläfer, M. Sievers, H. Klotzlicher and T. I. Onyeche, *Ultrasonics*, 2000, 38, 711–716.

- 53 B. E. Wood, H. C. Aldrich, and L. O. Ingram, *Biotechnol. Prog.*, 1997, 13, 232–237.
- 54 K. Suresh, A. Ranjan, S. Singh and V. S. Moholkar, *Ultrason. Sonochem.*, 2014, 21, 200–207.
- 55 W. L. Nyborg, *J. Acoust. Soc. Am.*, 1958, 30, 329–339.
- 56 S. Singh, S. T. P. Bharadwaja, P. K. Yadav, V. S. Moholkar and A. Goyal, *Ind. Eng. Chem. Res.*, 2014, 53, 14241–14252.
- 57 TAPPI, *Technical association of pulp and paper industry*. Atlanta, Georgia, USA, 1992.
- 58 A.J. Borah, M. Agarwal, M. Poudyal, A. Goyal, V.S. Moholkar, *Bioresour. Technol.* (2016) DOI: 10.1016/j.biortech.2016.02.024.
- 59 S. Singh, M. Agrawal, A. Bhatt, A. Goyal and V. S. Moholkar, *Bioresour. Technol.*, 2015a, 192: 636–645.
- 60 M. T. Holtzaple, *The pretreatment and enzymatic saccharification of Poplar wood*, Department of Chemical Engineering, University of Pennsylvania, USA, 1981.
- 61 M. T. Holtzaple, H. S. Caram and A. E. Humphrey, *Biotechnol. Bioeng.*, 1984, 26, 775–780.
- 62 N. Sreerama and R. W. Woody, *Anal. Biochem.*, 2000, 287, 252–260.
- 63 L. Whitmore and B. A. Wallace, *Nucleic Acid Res.* (Web Server Issue), 2004, 668–673.
- 64 L. Whitmore and B.A. Wallace, *Biopolymers*, 2008, 89(5), 392–400.
- 65 G. Davies and B. Henrissat, *Structure*, 1995, 3, 853–859.
- 66 J. Rouvinen, T. Bergfors, T. Teeri, J. K. C. Knowles and T. A. Jones, *Science*, 1990, 249, 380–386.
- 67 S. Singh, S. Sarma, M. Agrawal, A. Goyal and V. S. Moholkar, *Bioresour. Technol.*, 2015b, 188, 287–294.

- 68 G. P. Philippidis, D. D. Spindler and C. E. Wyman, *Appl. Biochem. Biotechnol.*, 1992, 34(35), 543–556.
- 69 D. S. Thomas and A. H. Rose, *Arch. Microbiol.*, 1979, 122, 49–55.
- 70 C. Leao and N. van Uden, *Biotechnol. Bioeng.*, 1982, 24, 2601–2604.
- 71 S. Singh, M. Agrawal, S. Sarma, A. Goyal and V. S. Moholkar, *Ultrason. Sonochem.*, 2015c, 26, 249–256.
- 72 R. Toegel, Reaction diffusion kinetics of a single sonoluminescing bubble. Ph.D. Dissertation, University of Twente, Netherlands, 2002.

Table 1: Summary of literature on ultrasound-assisted acid pretreatment (or dilute acid hydrolysis) of biomass

Reference	Biomass	Experimental Details	Major findings
Esfahani and Azin ⁹	Sugarcane bagasse	Time: 0-180 s; Sonication conditions: 20 kHz; 120 W Liquid medium: Sulfuric acid	94.49% sugar yield, optimum conditions: particle size < 0.18 mm, acid conc. 3% v/v, power 120 W, sonication time 180 s
Kunaver <i>et al.</i> ¹⁰	Wood waste	Time: 10–60 min; Sonication conditions: 24 kHz; 400 W; Liquid Medium: Water	4-9 fold reduction in liquefaction time of biomass in diethylene glycol/glycerol mixture with sonication with enhanced solubility.
Pejin <i>et al.</i> ¹¹	Triticale	Time: 5 min; Temperature: 313-333 K Sonication Condition: 40 kHz; 125 W Liquid Medium: Water.	Sonication improved glucose and maltose yield by 15.7% and 52.57%, respectively, and also increased bioethanol yield (SSF protocol) by 11%. Bioethanol yield: 0.43 g/g of triticale starch
García <i>et al.</i> ¹²	Olive tree pruning residues	Time: 30 -120 min; Temperature: 323 K Sonication conditions: 50-60 kHz; 420 W Liquid media: Acetic acid (organosolv treatment), NaOH (delignification) and water (autohydrolysis).	Ultrasound shows 10-20% rise in yield of reducing sugars, viz. glucose, xylose and arabinose and also removal of lignin. Lignin obtained in ultrasound assisted treatment did not suffer significant modifications in its physicochemical properties.
Harun <i>et al.</i> ¹³	Water hyacinth	Time: 10 – 30 min; Temperature: 303 K; Sonication conditions: 20 kHz; Liquid medium: Distilled water	Sugar yield (untreated sample): 24.7 mg sugar/ g dry matter; Steaming (121°C) and boiling (100°C) increases sugar yield by 36% and 52%; Highest sugar yield = 132.96 mg sugar/g dry matter with sonication for 20 min.
Nikolić <i>et al.</i> ¹⁴	Corn	Time: 1-10 min; Temperature: 333K Sonication conditions: 40 kHz	Increase in glucose concn. by 6.82% and 8.48% during pretreatment with ultrasound and microwave; Rise in ethanol concn. during SSF by 11% and 13% for ultrasound and microwave treatment.
Karki <i>et al.</i> ¹⁵	Hexane- defatted soybean flakes	Time: 15 – 120 s; Sonication conditions: 20 kHz; 2.2 kW; Liquid medium: Tap water	Sonication reduces particle size by 10 fold and increased total sugar release by 50% and total protein yield by 46% at high amplitude.
Nikolić <i>et al.</i> ¹⁶	Corn	Time: 1-30 min; Temperature: 333-353 K; Sonication conditions: 40 kHz; 600 W; Liquid medium: Water	Sugar yield increased by 7% with sonication. Max ethanol concentration (SSF treatment) of 9.67% w/w with sonication (11.15% augmentation).
Yunus <i>et al.</i> ¹⁷	Oil palm empty fruit bunch (OPEFB)	Time: 15 -60 min; Temperature: 298 K Sonication conditions: 20 kHz; 2 kW; Liquid medium: Sulfuric acid	3-fold increase in xylose yield was obtained with sonication at 100°C; No distinct effect of sonication on increment in xylose yield for treatment at 120 and 140°C.
Nitayavardhana <i>et al.</i> ¹⁸	Cassava chips	Time: 10-30 s; Temperature: 323K; Sonication conditions: 20 kHz; 2.2 kW; Liquid medium: Acetate buffer at pH 4.8	40-fold reduction in cassava particle size with sonication. Sonication reduces fermentation time by 24 h with 2.7 fold increase in bioethanol yield; Reducing sugar yield = 22 g / 100 g of samples
Aimin <i>et al.</i> ¹⁹	Eucalyptus cellulose fiber	Time: 0-720 s; Sonication conditions: 23-25 kHz; 400 W; Liquid medium: Sodium periodate	Change in morphology, accessibility and oxidation reactivity of cellulose with sonication. Increase in cellulose accessibility (73-119%) without much change in structure.

Table 2: Summary of literature on ultrasound-assisted alkaline pretreatment (or delignification) of biomass

Reference	Biomass	Experimental Details	Major findings
Bussemaker <i>et al.</i> ²⁰	Wheat straw	Temperature: 328 K; Sonication conditions: 40, 376 and 995 kHz; Liquid medium: water	Delignification was favored at frequency of 40 kHz (7.2%) and carbohydrate solubilization (9.1%) was favored at 995 kHz.
Baxi and Pandit ²¹	Wood	Temperature: 303 K Sonication condition: 22 kHz; 240 W	Lignin content of wood reduced to required value, at room temperature and low pressure, using hydrodynamic cavitation.
Sasmal <i>et al.</i> ²²	Areca nut husk, Bon bogori and Moj (<i>Albizia lucida</i>)	Time: 60-180 min; Temperature: 308 K; Sonication conditions: 30 kHz, 100 W; Liquid medium: Lime solution	% delignification and bioethanol concn. by SSF of ultrasound pretreated biomass: Areca nut husk – 65%, 22.5 g/L; Bon bogori – 68%, 34.4 g/L; Moj (<i>Albizia lucida</i>) – 64%, 39.1 g/L
Velmurugan and Muthukumar ²³	Sugarcane bagasse	Time: 20 min; Temperature: 323K Sonication conditions: 25 kHz; 400 W Liquid Medium: NaOH (2%)	Sono-assisted alkali pretreatment removed 81% lignin and 91% hemicellulose. Optimum conditions: reaction time – 360 min, liquid to solid ratio – 15:1, cell mass – 15 g/L.
Velmurugan and Muthukumar ²⁴	Sugarcane bagasse	Time: 5-50 min; Temperature: 343 K Sonication conditions: 25 kHz; 400 W Liquid Medium: NaOH	Max. sugar yield under optimum conditions: 92.1% Substantial reduction in pretreatment time and temperature with improved efficiency with ultrasound-assisted alkaline pretreatment.
Chen <i>et al.</i> ²⁵	Poplar wood	Time: 1-2 h; Temperature: 338 – 343 K Sonication conditions: 20-25 kHz; 400-1200 W Liquid medium: 3-6 wt % KOH	5-20 nm ranged nanofibers obtained with hemicellulose and lignin removed extensively and crystallinity of 69%
Velmurugan and Muthukumar ²⁶	Sugarcane bagasse	Time: 15-75 min; Temperature: 323K Sonication conditions: 24 kHz Sono-assisted alkaline pretreatment	Cellulose & hemi-cellulose recovery – 99% & 79%, lignin removal 75%. Very low inhibitor content in hydrolyzate. Bioethanol yield = 0.17 g/g of pretreated sugar cane bagasse
Yuan <i>et al.</i> ²⁷	Poplar wood	Time: 30 min, 3 h; Temperature: 298 & 348 K Sonication conditions: 20-24 kHz; 570 W Liquid Media: Ethanol, dimethyl sulfoxide, NaOH	Sonication / extraction with NaOH releases 96% lignin and 75.5% hemicellulose. Purified hemicellulosic fractions contain low amount of associated lignin.
Zhang <i>et al.</i> ²⁸	Corn	Time: 48 h; Temperature: 298 K; Sonication conditions: 4 kHz; 80 W; Liquid Medium: NaOH	No change in surface conformation of granular raw material by sonication. Increase in catalytic efficiency of cellulase by 70% and 44% lignin removal with sonication.
Sun <i>et al.</i> ²⁹	Sugarcane Bagasse	Time: 40 min; Temperature: 328 K; Sonication conditions: 20 kHz; 100 W; Liquid Medium: Distilled water at pH 11.5	> 90% extraction of hemicellulose and lignin in proglinal biomass with ultrasound. No change in structure of hemicellulosic fraction – which comprised <i>L-arabino(4-<i>o</i>-metnyl-<i>D</i>-glucurono)-<i>D</i>-xylans</i> .
Sun <i>et al.</i> ³⁰	Wheat straw	Time: 5 – 35 min; Temperature: 333K; Sonication conditions: 20 kHz; 100 W; Liquid Medium: NaOH in 60% aqueous methanol	Increase in hemicellulose yield: 2.9-9.2% for 5-35 min sonication. Hemicelluloses isolated with sonication had relatively lower molecular weight and more linearity.
Sun and Tomkinson ³¹	Wheat straw	Time: 5 – 35 min; Temperature: 308 K; Sonication conditions: 20 kHz; 100 W; Liquid Medium: KOH	Lignin removal: 43.9-49.1% for ultrasound treatment for 5-35 min. High purity of lignin with ultrasonic treatment with lower content of polysaccharides.

Table 3: Summary of literature on ultrasound-assisted enzymatic hydrolysis of biomass

Reference	Biomass	Experimental Details	Major findings
Bharadwaja <i>et al.</i> ³²	<i>Parthenium hysterophorus</i>	Time: 4 h; Temperature: 303 K; Sonication conditions: 35 kHz, 35 W; Optimization of enzyme hydrolysis using RSM.	Sonication gives 18-fold enhancement in kinetics of hydrolysis. Total ethanol yield from fermentation of pentose and hexose hydrolyzates = 0.26 g/g raw biomass.
Sulaiman <i>et al.</i> ³³	Carboxymethyl cellulose (CMC) and insoluble cellulose	Time: 20 min; Temperature: 323 K Sonication conditions: 10, 20 and 40% duty cycle. Liquid Medium: acetate buffer, pH: 4.8	Optimum duty cycle: 10% for 2-fold higher reaction rate. Increase in max reaction rate V_{\max} with reduction in Michaelis constant K_m . Loss of enzyme activity with sonication.
Li <i>et al.</i> ³⁴	Sugarcane bagasse	Time: 20 -40 s; Temperature: 363 K; Sonication Condition: 45 kHz; 100 W; Liquid medium: aq. N-methyl morpholine-N-oxide (NMMO)	NMMO-treated cellulose under ultrasound was porous and amorphous that assists saccharification. Sonication resulted in higher hydrolysis (96.5%) of biomass.
Ninomiya <i>et al.</i> ³⁵	Kenaf core fiber	Time: 0-120 min; Temperature: 298 K; Sonication conditions: 24 kHz; 35 W; Liquid media: Ionic liquids	60 – 95% cellulose hydrolysis to glucose in ionic liquids at 25°C. Cellulose saccharification ratio in ionic liquid EmimOAc = 86% for 15 min ultrasound pretreatment at 25°C.
Karki <i>et al.</i> ³⁶	Extruded Full fat soybean flakes	Time: 30 -60 s; Sonication conditions: 20 kHz; 2.2 kW; Liquid medium: Sodium acetate buffer	No rise in saccharification yield 30 and 60 s sonication of insoluble fraction.
Montalbo-Lomboy <i>et al.</i> ³⁷	Corn	Time: 5 -40 s; Sonication conditions: 20 kHz; Liquid medium: Acetate buffer; Hydrolysis of starch using α -amylase and gluco-amylase	3-fold increase in sugar release with sonication of the maize mash. Partial gelatinization of sugary starch during sonication. Increase in activity of the enzymes during sonication.
Yang <i>et al.</i> ³⁸	Microcrystalline cellulose	Time: 30 min; Temperature: 333 K; Sonication conditions: 45 kHz; 100 W; Liquid medium: Alkylphosphate ionic liquids (aq. media)	>95% conversion of cellulose to glucose in aq. Mmim Dimethyl phosphate with sonication. Ionic liquid-treated cellulose undergoes depolymerization with sonication that assists saccharification.
Shewale and Pandit ³⁹	Three different types of sorghum grains	Time: 1 min; Sonication conditions: 20 kHz; 750 W. Liquid medium: Acetate buffer and Citrate buffer pH: 4.5 and 5.5	Sonication increases saccharification by 8% and reduces particle size by 50%. Higher availability of additional starch for hydrolysis due to ultrasound-assisted disruption of the protein matrix.
Yu <i>et al.</i> ⁴⁰	Rice hull	Time: 10-60 min; Temperature: 298 K Sonication conditions: 40 kHz; 250 W	Pretreatment combining sonication + H ₂ O ₂ followed by biological treatment. Higher lignin degradation and increase in total reducible sugar yield.
Khanal <i>et al.</i> ⁴¹	Corn slurry	Time: 20-40 s; Sonication conditions: 20 kHz; 2.2 kW, Liquid medium: Acetate buffer and water.	Enhanced enzyme activity but did not denature the enzymes. 20-fold particle size reduction, 2-fold increase in total sugar release
Li <i>et al.</i> ⁴²	Waste paper	Temperature: 318 K; Sonication conditions: 20 kHz; 250 W, Liquid medium: Acetate buffer at pH 4.8	Enhancement of saccharification of wastepaper with ultrasound.
Imai <i>et al.</i> ⁴³	Carboxymethyl cellulose	Time: 30 min; Temperature: 323 K; Sonication conditions: 135 W; Liquid medium: Acetate buffer,	Pretreatment of cellulose fibers with sonication before enzymatic hydrolysis improved the hydrolysis reaction rate.
Li <i>et al.</i> ⁴⁴	Paper pulp	Time: 48 h; Temperature: 318 K; Sonication conditions: 20 kHz; 30 W; Liquid medium: Acetate buffer	Crystallinity and residual lignin of pulp affect saccharification rate. Sonication increases the reaction velocity of hydrolysis – but no effect on K_m and competitive product inhibition constants.

Table 4: Kinetic/physiological parameters of HCH-1 model for enzymatic hydrolysis of *Parthenium hysterophorous* (Reproduced from Singh *et al.*⁵⁹ with permission of Elsevier BV).

(A) Lineweaver-Burk analysis (enzyme kinetic parameters)		
Experiment	K_m (g/L)	V_{max} (mM/min)
Control (mechanical agitation)	42.77	0.046
Test (with ultrasound)	24.44	0.055
(B) Analysis with HCH-1 model with GA optimization		
Parameter	Control experiment (mechanical agitation)	Test experiment (with ultrasound)
Lumped kinetic constant of enzymatic hydrolysis, κ (h ⁻¹)	0.31	1.22
Lumped constant for enzyme/ substrate complexation, α (g/L)	0.49	0.19
Product binding constant, β (L/g)	1.01	0.76
Number of cellulose sites covered by adsorbed or complexed enzyme, ϕ	0.17	0.19
Best fitness value for the model parameters	5.71	4.3

Table 5 (A): Composition of the secondary structure of native and ultrasound treated enzymes for biomass hydrolysis (Reproduced from Borah *et al.*⁵⁸ with permission of Elsevier BV).

Results for cellulase enzyme				
Form of cellulase enzyme	α -helix (%)	β -sheet (%)	β -turn (%)	Random coil (%)
1. Native Enzyme	32.7	13.20	23.1	30.8
2. Enzyme treated with mechanical shaking	30.67	25.24	18.54	25.53
3. Enzyme treated with sonication (at atmospheric conditions)	19.10	29.75	18.40	32.73
Results for cellobiase enzyme				
1. Native Enzyme	11.68	44.46	10.23	33.71
2. Enzyme treated with mechanical shaking	9.84	45.5	10.76	33.5
3. Enzyme treated with sonication (at atmospheric conditions)	9.85	45.6	10.77	33.7
Results for mixture of cellulose and cellobiase enzymes				
1. Native Enzyme	33.04	11.46	23.89	31.69
2. Enzyme treated with mechanical shaking	32.88	11.63	23.84	31.73
3. Enzyme treated with sonication (at atmospheric conditions)	32.08	11.87	24.04	31.99

Table 5 (B): Kinetic/ physiological parameters of the HCH-1 model for enzymatic hydrolysis of invasive biomass species (Reproduced from Borah *et al.*⁵⁸ with permission of Elsevier BV).

Biomass species	Control experiment (mechanical agitation)					Test experiment (under sonication)				
	κ	A	β	ε	F -best	κ	A	β	ε	F -best
SS	0.51	0.31	0.21	0.10	4.60	1.98	0.26	0.12	0.11	6.10
LC	1.05	0.49	0.79	0.03	5.00	1.69	0.35	0.32	0.04	5.60
EC	1.01	0.34	0.56	0.14	4.60	1.85	0.25	0.25	0.15	4.76
MM	0.38	0.55	0.33	0.11	3.40	1.66	0.42	0.28	0.10	4.20

Notation: κ – Lumped kinetic constant of enzymatic hydrolysis (h^{-1}); α – Lumped constant for enzyme–substrate complexation (g/L); β – Product binding constant (L/g); ε – Number of cellulose sites covered by adsorbed or complexed enzyme; F -best – Best fitness value for the model parameters

Table 6: Kinetic and physiological parameters for simultaneous saccharification and fermentation (SSF) of *Parthenium hysterophorous* (Reproduced from Singh *et al.*⁷¹ with permission of Elsevier BV).

Parameter	Control Experiments	Test Experiments
Monod constant for cell growth, K_3 (g/L)	25.01	20.02
Inhibition constant of cell growth by glucose, K_i (g/L)	50.06	60.02
Inhibition constant of cell growth by ethanol, K_{3E} (g/L)	30.03	30.01
Specific cell death rate, k_d (1/h)	0.12	0.09
Maximal specific growth rate, μ_m (1/h)	0.48	0.61
Constant for growth associated ethanol formation, a (g/g)	2.98	2.99
Non-growth associated specific ethanol production rate, b (g/g/h)	1.99	1.99

Table 7: Summary of simulations of cavitation bubble dynamics (Reproduced from Singh *et al.*⁷¹ with permission of Elsevier BV)

Parameters for simulations		
Water		
	Air bubble	Air bubble
	$R_o = 5 \mu\text{m}$	$R_o = 10 \mu\text{m}$
Conditions at the first collapse of the bubble		
Species	$T_{\text{max}} = 3258 \text{ K}$	$T_{\text{max}} = 2304 \text{ K}$
	$P_{\text{max}} = 384 \text{ MPa}$	$P_{\text{max}} = 88.4 \text{ MPa}$
	$V_{\text{turb}} = 0.03 \text{ mm/s}$	$V_{\text{turb}} = 0.05 \text{ mm/s}$
	$P_{\text{AW}} = 72 \text{ kPa}$	$P_{\text{AW}} = 31.6 \text{ kPa}$
Equilibrium composition of bubble at transient collapse		
N ₂	7.1952E-01	7.0137E-01
O ₂	1.6608E-01	1.8081E-01
O	1.6723E-03	7.2220E-05
O ₃	6.4788E-06	—
H	7.1808E-05	1.3605E-06
H ₂	1.8629E-04	1.6934E-05
NO	5.6173E-02	1.4597E-02
NO ₂	1.3272E-03	4.1249E-04
N ₂ O	1.7158E-04	2.0512E-05
OH	7.3692E-03	1.3447E-03
H ₂ O	4.6767E-02	1.0124E-01
HO ₂	4.3753E-04	7.0556E-05
H ₂ O ₂	2.6760E-05	5.7095E-06
HNO	2.2534E-05	—
HNO ₂	1.646E-04	3.6992E-05

Note: Conditions for simulations: Ultrasound frequency = 35 kHz; Ultrasound pressure amplitude = 150 kPa; Equilibrium bubble radius = 5 and 10 μm ; Vapor pressure of water (in bar) is calculated using Antoine type correlation: $\log_{10} P_v = 3.55959 - \frac{643.748}{T - 198.043}$. Properties of water: density = 1000 kg/m^3 , kinematic viscosity = 10^{-6} $\text{Pa}\cdot\text{s}$, surface tension = 0.072 N/m and sonic velocity = 1481 m/s .

Notation: R_o – initial radius of the cavitation bubble; V_{turb} – average velocity of the micro-turbulence in the medium generated by cavitation bubbles in the medium (estimated at 1 mm distance from bubble center); P_{AW} – pressure amplitude of the acoustic wave generated by the cavitation bubble (estimated at 1 mm distance from bubble center); T_{max} – temperature peak reached in the bubble at the time of first collapse; P_{max} – pressure peak reached in the bubble at the time of first collapse

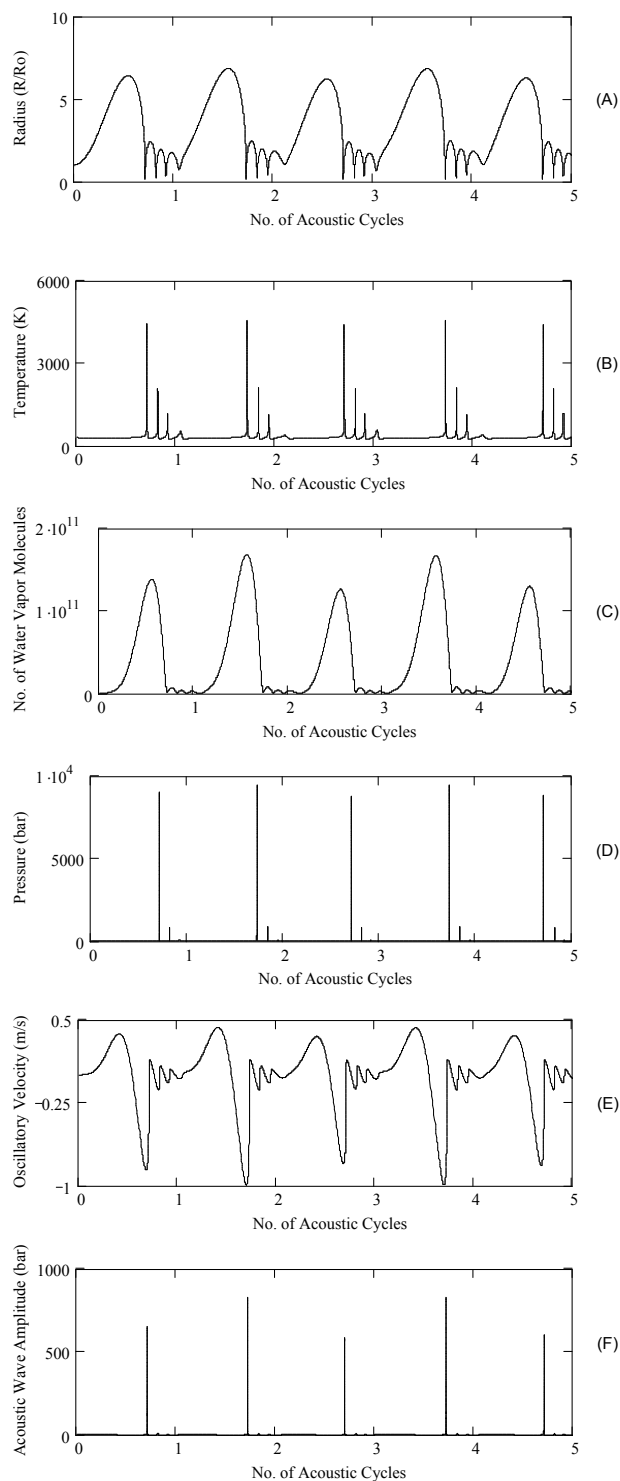


Figure 1. Representative simulation results (5 μm air bubble at 303 K, NaOH conc. 1.5% w/v). Time variation of (A) normalized bubble radius (R/R_0); (B) temperature in the bubble; (C) number of water molecules in the bubble; (D) pressure inside the bubble; (E) micro-turbulence generated by the cavitation bubble; (F) acoustic (or shock) waves emitted by the bubble (Reproduced from Singh *et al.*⁵⁶ with permission of American Chemical Society)

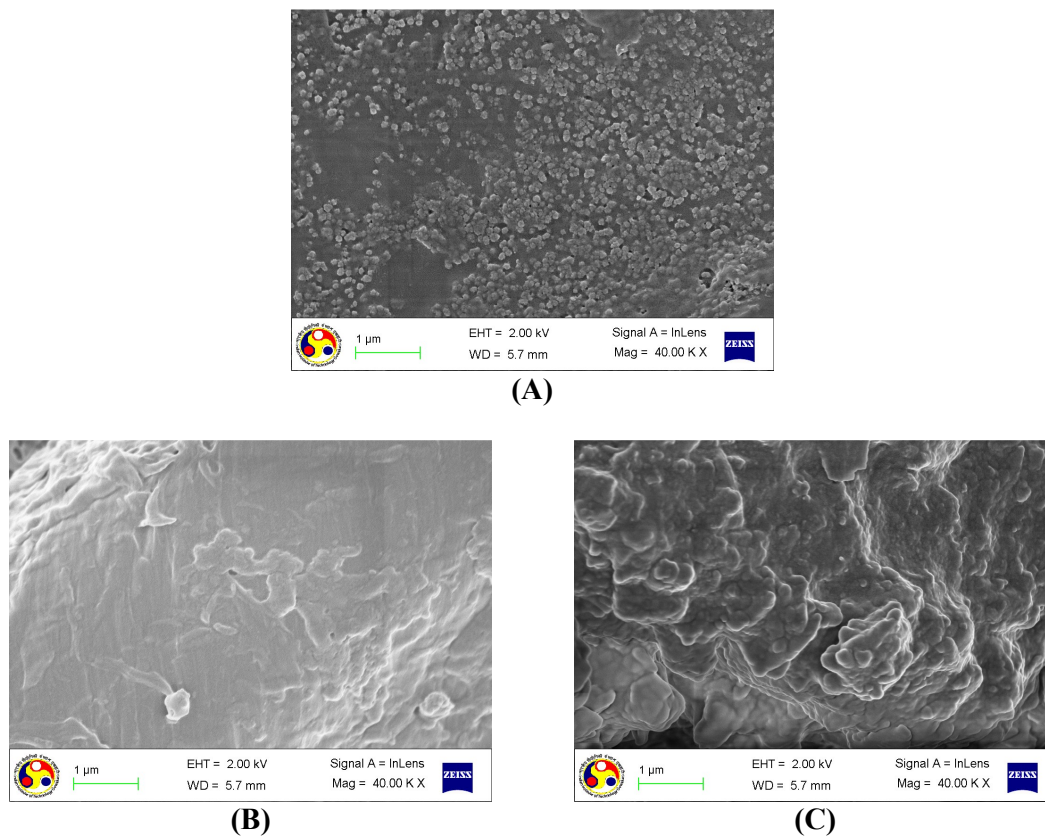


Figure 2. FESEM micrographs of *P. hysterothorus* biomass (A) pretreated biomass, (B) delignified biomass with mechanical agitation, and (C) delignified biomass with ultrasound. (Reproduced from Singh *et al.*⁵⁶ with permission of Elsevier BV)

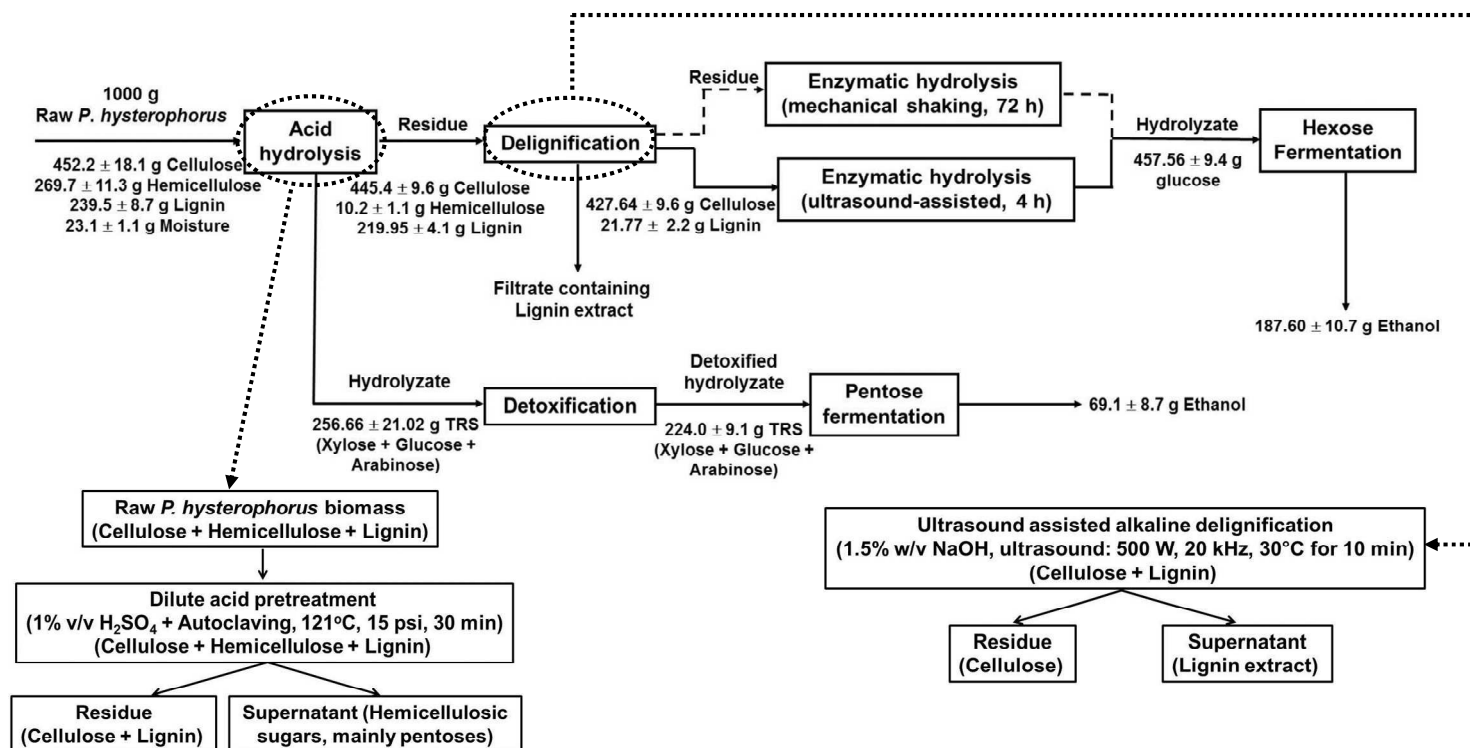


Figure 3. Conceptual process for bioethanol production from *P. hysterophorus*: Flow sheet with complete mass balance (Reproduced from Bharadwaja *et al.*³² with permission of Elsevier BV).

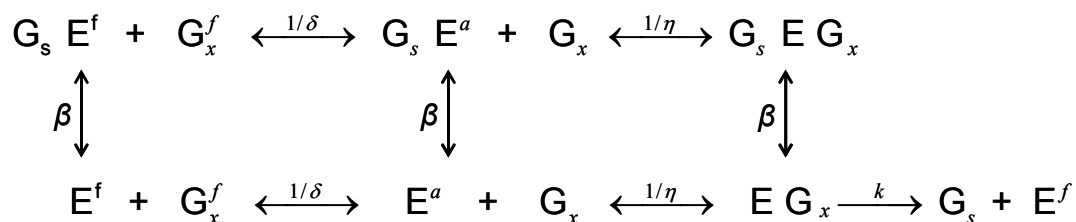


Figure 4 (A). Reaction mechanism for the HCH-1 model (Reproduced from Singh *et al.*⁵⁹ with permission of Elsevier BV)

(**Notation:** G_x^f - free cellulose, G_x - cellulose site, G_s - soluble product, E^f - free enzyme, E^a - enzyme adsorbed on cellulose, EG_x - enzyme substrate complex, $G_s E^f$ - inhibited free enzyme, $G_s E^a$ - inhibited adsorbed enzyme, $G_s E G_x$ - inhibited complexed enzyme, η - complexing constant, β - product binding constant, δ - adsorption constant, k - reaction rate constant)

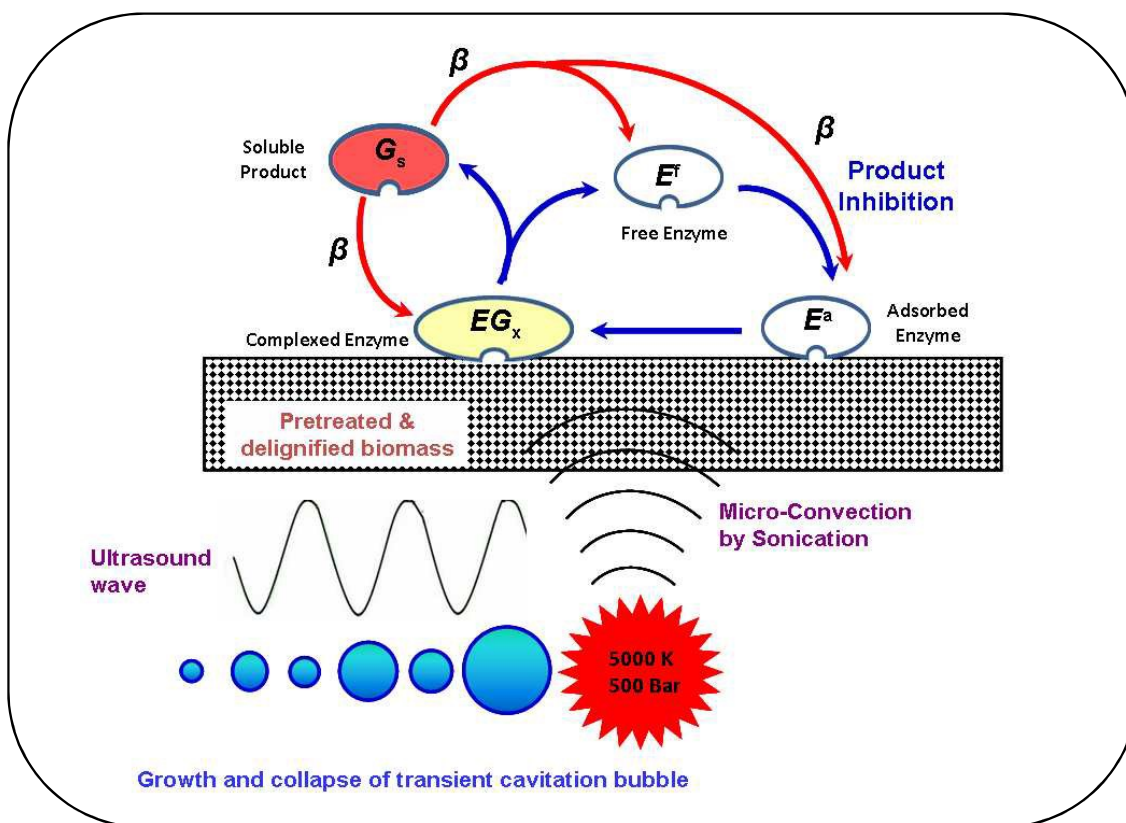


Figure 4 (B). Schematic of the ultrasound-assisted enzymatic biomass hydrolysis (Reproduced from Singh *et al.*⁵⁹ with permission of Elsevier BV).

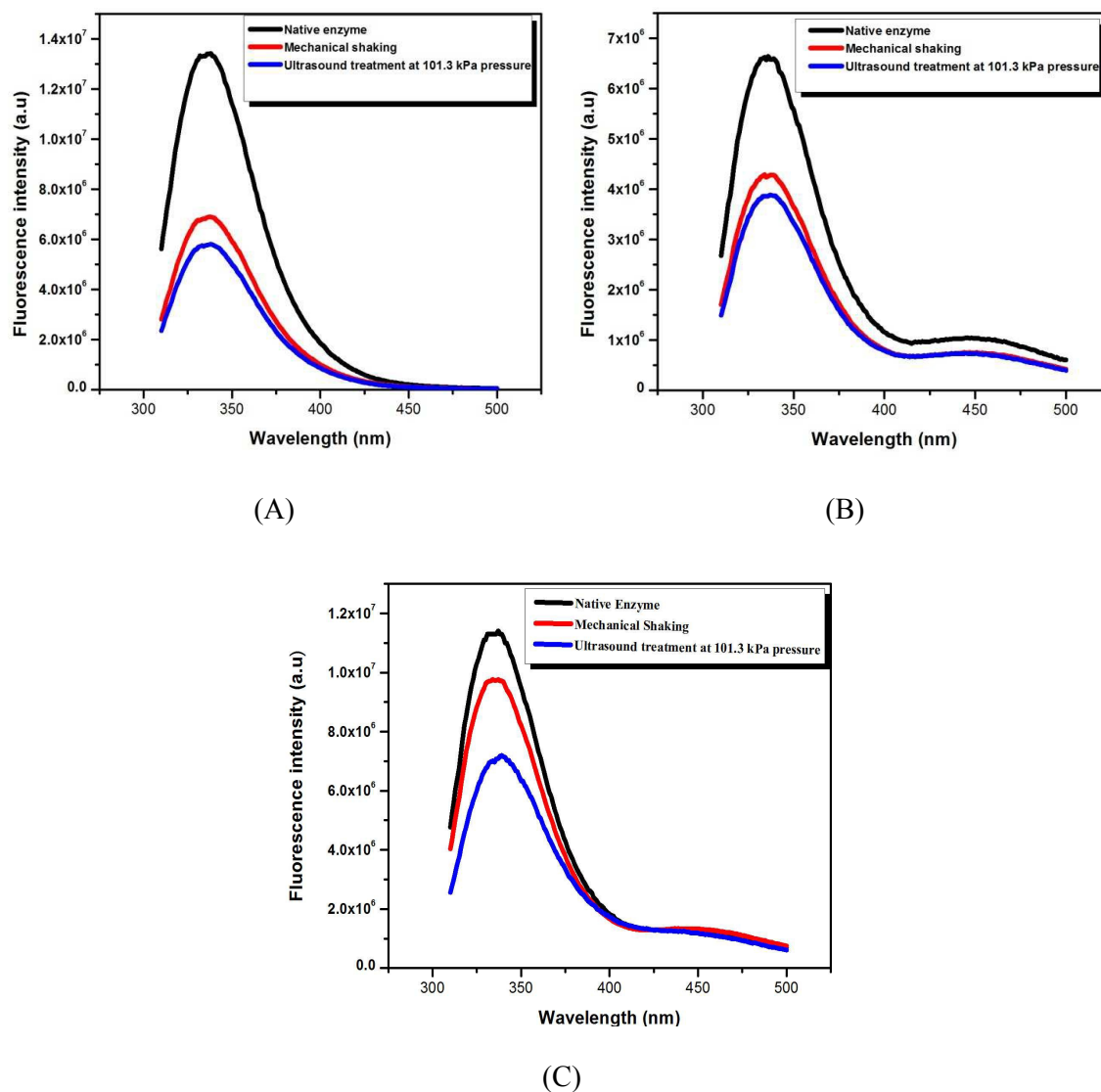


Figure 5. Intrinsic fluorescence spectra of hydrolysis enzymes in various forms (native enzyme and post-treatment with mechanical shaking and sonication at atmospheric or 101.3 kPa pressure). (A) Spectra of cellulase enzyme; (B) Spectra of cellobiase enzyme; (C) Spectra of mixture of cellulase and cellobiase enzymes (Reproduced from Borah *et al.*⁵⁸ with permission of Elsevier BV)

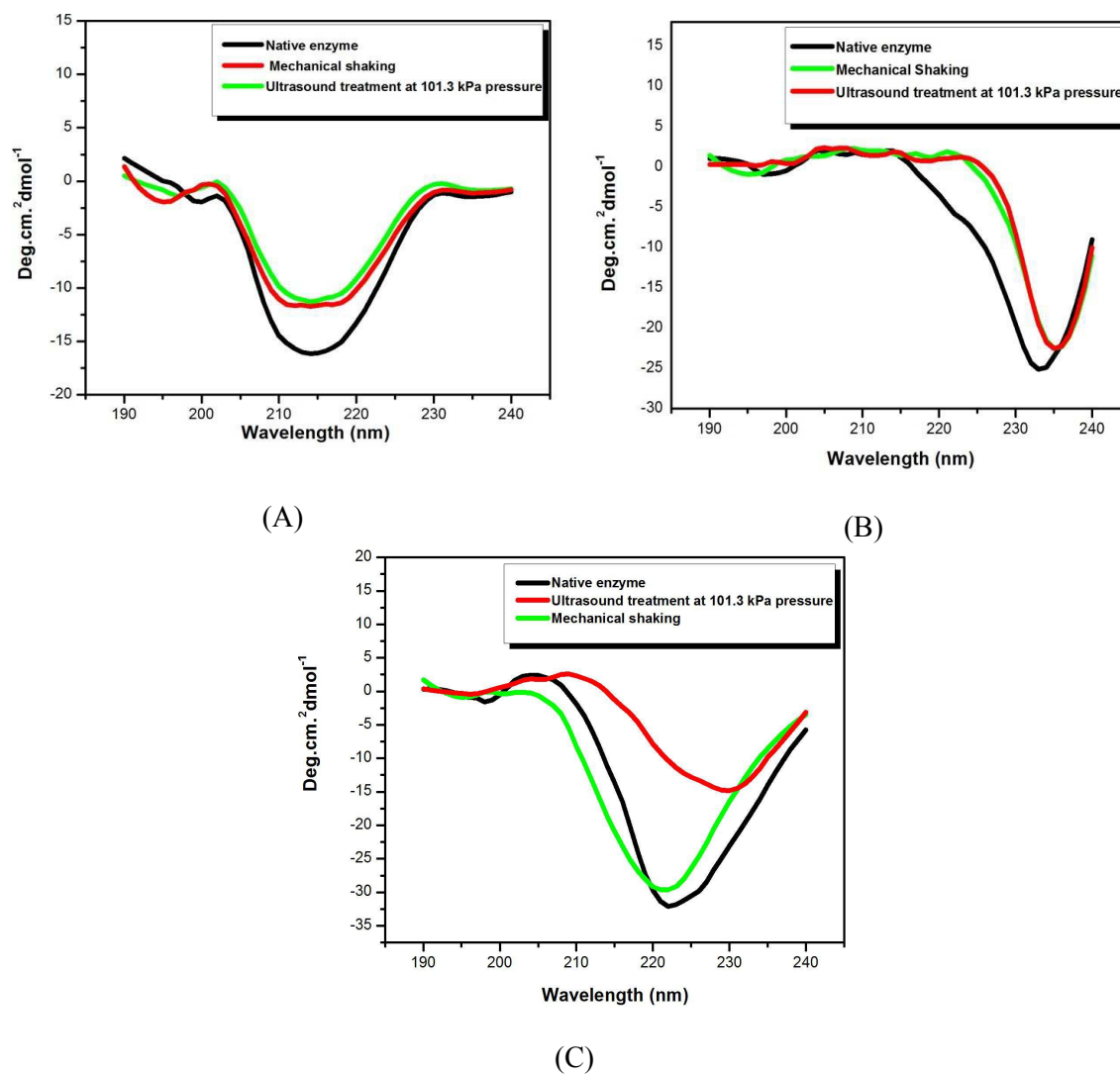


Figure 6. Circular dichroism spectra of hydrolysis enzymes in various forms (native enzyme and post-treatment with mechanical shaking and sonication at atmospheric or 101.3 kPa pressure). (A) Spectra of cellulase enzyme; (B) Spectra of cellobiase enzyme; (C) Spectra of mixture of cellulase and cellobiase enzymes (Reproduced from Borah *et al.*⁵⁸ with permission of Elsevier BV)

